Telemark University College
Faculty of technology
M.Sc. Programme

MASTER THESIS 2007

Candidate : Hilde Andersen

Title : Computational study of heat transfer in subsea deadlegs for evaluation of possible hydrate formation

Faculty of Technology
Address: Kjolnes Ring 56, N-3914 Porsgrunn, Norway, tel: +47 35 57 50 00, fax: +47 35 55 75 47

Telemark University College

Faculty of Technology

M.Sc. Programme

WRITTEN REPORT MASTER THESIS, COURSE CODE F4203

Student	:	**Hilde Andersen**
Thesis Title	:	**Computational study of heat transfer in subsea deadlegs for evaluation of possible hydrate formation**
Signature	:	
Number of pages	:	**55**
Keywords	:	**Subsea deadleg, heat transfer, CFD simulations, hydrate, Fluent**

Supervisor	:	**Knut Vågsæther**	sign:
Sensor	:	**Vidar Mathiesen**	sign:
External partner	:	**Audun Faanes, Statoil ASA**	
Availability	:	**Open**	
Archive approval	:		**Date:**

Abstract:

The background for this project is the request of achieving more knowledge of the temperature and velocity fields in different subsea deadleg geometries. This is important to avoid hydrate formation in subsea equipment. The literature review revealed only a few studies on this topic. Two studies on corrosion, both experimental and numerical, in subsea deadlegs where performed by Habib. Results show almost stagnant flow 3-4 D_i into the deadleg.

To study the heat transfer in such systems, two deadlegs was modeled in Fluent, a vertical and a horizontal oriented deadleg. The choice of geometry and some input data is based on the former work done by IFE and Habib and his crew. The simulations where run with two different velocities and outer heat transfer coefficient. The effect of buoyancy in the vertical deadleg is also investigated. The results shows that the vertical deadleg has a more abrupt temperature profile outwards in the deadleg than the horizontal. For tree of the eight cases, the temperature crosses the HET (hydrate equilibrium temperature) and is therefore in the temperature range where hydrates will start to form. To be able to suggest a design criterion for subsea deadlegs, this problem should be further investigated.

PREFACE

This is a report from the main thesis in the master program at Telemark University College. Through the main thesis the student is expected to gain experience and knowledge with regard to individual, scientific work. The student is attending the Process Technology master program. The main thesis incorporates both experimental and theoretical work and is carried out on an individual basis.

I would like to thank Mr. Audun Faanes at the Statoil research center in Trondheim for the positive response, and he has done a great job in organizing this project and helping me to get in touch with the right people. For the CFD part, Mr. Carl Birger Jenssen and Mrs. Bente Helgeland Sannæs have been most helpful and they have contributed with their knowledge and experience. I learnt a lot during the two days I spent with them in Trondheim. Bente was also so kind and ran the buoyancy simulation for me. Stian Solbakken, Statoil Stavanger, provided the task background and a previous study that has been the basis for the CFD simulations.

I will also thank my supervisor at Telemark University College, Mr. Knut Vågsæther for good guidance and answering all my questions with a great deal of patience.

Finally, I will thank my husband for the support through these five years.

Porsgrunn, June 1, 2007

Hilde Andersen

INDEX

LIST OF FIGURES

NOMENCLATURE

Abbreviations

HET	-	hydrate equilibrium temperature
HTC	-	heat transfer coefficient
MEG	-	mono ethylene glycol

Letters and expressions

A	-	area	[m^2]
C_p	-	heat capacity	[kJ/kg·K]
c	-	circumference	[m]
D	-	diameter	[m]
D_i	-	inner diameter	[m]
E	-	energy	[J]
g	-	gravity acceleration	[m/s^2]
$\dot{H}$	-	rate of enthalpy	[kJ/kg·s]
h	-	convection heat transfer coefficient	[W/m^2K]
h	-	enthalpy	[kJ/kg]
j	-	species	
k	-	thermal conductivity	[W/m·K]
L	-	characteristic length	[m]
Nu	-	Nusselts number,	
Pr	-	Prandtl number, ratio of momentum diffusivity to thermal diffusivity	
p	-	pressure	[Pa]
q	-	heat transfer rate	[W]
q''	-	heat flux	[W/m^2]
$\dot{Q}$	-	heat transfer rate	[W]
Ra	-	Rayleigh number, measure of the strength of buoyancy-induced flow in	

free convection)

Re	-	Reynolds number	
S	-	surface area	[m^2]
S_h	-	source term	
T	-	temperature	[K]
T_{sea}	-	sea temperature	[K]
ΔT_{LM}	-	temperature difference, logarithmic mean	[K]
T	-	time	[s]
U	-	overall heat transfer coefficient	[W/m^2K]
U_i	-	internal energy	[J]
V/v	-	fluid velocity	[m/s]
W	-	work	[W]
Y_j	-	mass fraction of species j	

Greek letters

θ	-	angle	[degrees]
ρ	-	density	[kg/m^3]
μ	-	dynamic viscosity	[kg/s·m]
ε	-	epsilon	
ν	-	kinematic viscosity	[m^2/s]
α	-	thermal diffusivity	[m^2/s]
σ	-	temperature difference	[K]
β	-	coefficient of expansion	[$1/^oC$]
$\bar{\bar{\tau}}$	-	Stress tensor	[Pa]

1 INTRODUCTION

This report is a computational and analytical study of hydrate formation in subsea systems. There are a number of challenges connected to hydrates and subsea production. The first part of the report is a literature review on heat transfer systems and hydrates. The literature review also includes modeling theory and equations. Chapter three describes the development of the CFD model, followed by the results in chapter four and discussion in chapter five.

1.1 Background

Hydrate formation in hydrocarbon production systems is a well known challenge for the oil and gas industry. Hydrate formation is undesired and may cause production loss, equipment damage/integrity and personnel injuries. In order to minimize the probability of hydrate formation, the equipment design is an important factor, combined with process properties. Maintaining the process fluid temperature above a threshold-value, referred to as the hydrate equilibrium temperature, effectively protects the system from hydrate formation. Subsea production systems are generally more exposed due to unfavorable ambient conditions, i.e. cold surroundings and sea currents which favor a large heat loss. Deadlegs, i.e. piping without through-put, are of special concern since fluid temperatures in such devices typically drops abruptly towards the dead-end. It is of crucial importance to keep dead-legs above the hydrate formation temperature during production. Deadlegs are commonly found in relation with chemical injection lines and on manifolds. Future subsea production systems will increase in complexity, and accordingly more deadlegs will be introduced in such systems. From a hydrate-protection point of view this is challenging. The design of subsea production systems involving deadlegs should as far as possible be governed by hydrate-protection requirements to minimize hydrate related problems. In order to achieve an improved design of deadlegs more knowledge regarding the temperature distribution in deadlegs is needed.

1.2 Objectives

The objectives of this project are

- To study a subsea oil and gas production system to achieve knowledge and understand the challenges associated with such systems and to obtain typical process parameters for the CFD simulations. The Tordis oil and gas production system will be utilized for this purpose.
- To review and make a summary of literature on heat transfer and flow patterns due to natural convection with focus on subsea deadlegs.
- To perform a simplified analytical analysis of these effects.

- To set up and perform CFD (Computational Fluid Dynamics) study of heat transfer effects in subsea deadlegs. The tools for the CFD study are Fluent for the numerical solution and Gambit for developing the geometry and grid.
- To evaluate the possibility of hydrate formation in subsea deadlegs based on the results from the CFD study, and consider the possibility of suggesting a design criterion for subsea deadlegs.

1.3 Motivation

The motivation for this project is to investigate heat transfer effects in subsea equipment for oil and gas production. Traditionally oil and gas in the North Sea has been produced and processed from big and expensive drilling and production platforms, with all the equipment placed topside. To lower installation cost and make smaller projects cost-effective, subsea solutions with topside or subsea processing is now the preferred way of developing a new oilfield. This leads to different design and operating challenges to make subsea production possible. To achieve flexible solutions the geometries are more complex and the possibility of hydrate formation in deadlegs increased.

1.3.1 Deadleg

According to [9], deadleg is a term used to describe the inactive part of a pipe. The deadleg is a part of a pipe system with low velocity to stagnant flow, e.g. by-passes, chemical injection lines, optional routing of flow. They are also referred to as branches, and are connected to an active pipe carrying the main stream. These deadlegs or branches are vulnerable to hydrate formation and corrosion. It is important to consider the deadleg geometry in the design phase of subsea equipment in such a way that the fluid temperature never crosses the hydrate equilibrium curve. There are several possible geometries; some examples are given in Figure 1-1. The arrows indicate the direction of the main flow.

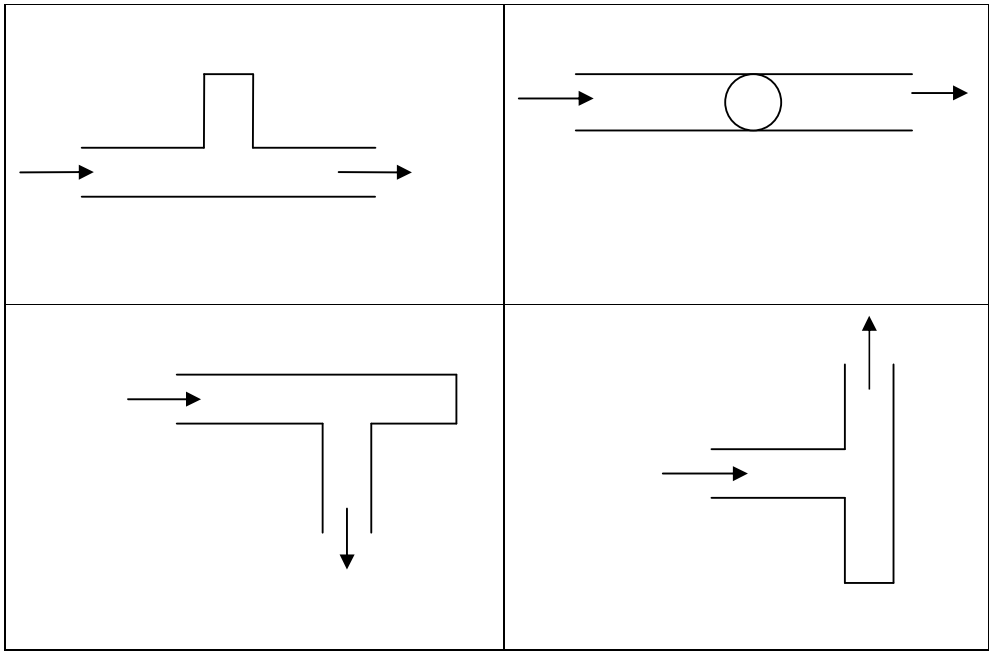

Figure 1-1: Examples of deadleg geometries

1.4 The Tordis subsea production system

To understand the complexity and how a subsea production system is designed, the Tordis field will be described and used as an example of a typical case. The Tordis field was designed and built by the oil company Saga Petroleum in 1994. The chosen solution for this field was a subsea production system consisting of satellite well equipment, subsea manifold and control system. From the subsea manifold, two parallel pipelines for transportation of the well stream to the Gullfaks C platform and further processing topside. Since the start-up in 1994 another two templates has been connected to the subsea manifold. Figure 1-2 shows a overview of the existing Tordis production system. The distance from the Gullfaks C platform is about 12 km. The subsea manifold with satellite wells and J-template are for oil production wells, and the K-template contains water injection wells. The dotted lines show the placing of the new PLIM (pipeline inline manifold), SSS (subsea separator) and the Utsira water injection well. The SSS is under construction and the planned start-up for this system is fall 2007.

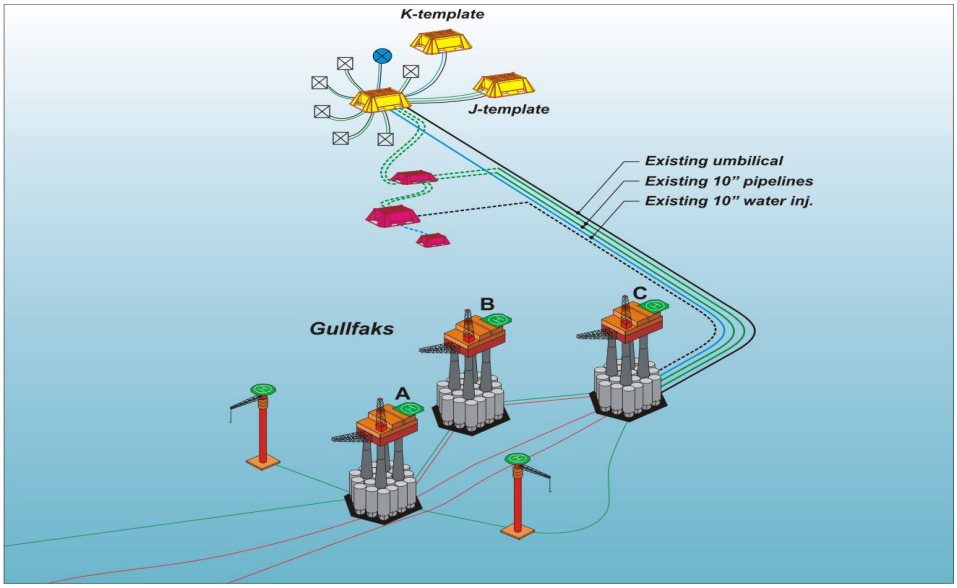

Figure 1-2: Overview of the Tordis subsea production system and processing platform [14]

Figure 1-3 shows the future Tordis subsea processing system with the new SSS, PLIM and water injection well.

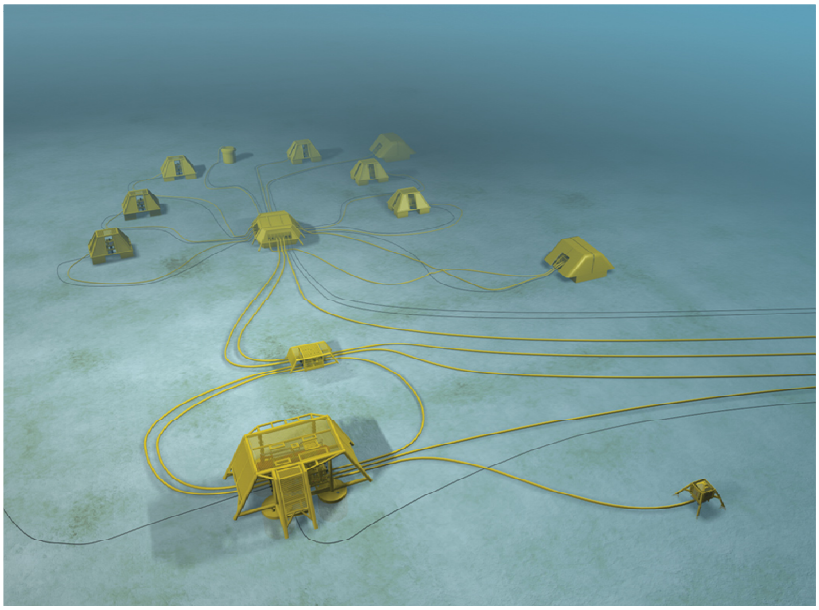

Figure 1-3: Future Tordis subsea separator [14]

1.4.1 Satellite wells

The Christmas tree and control module is placed inside of a protection frame which protects the equipment against trawling equipment and falling loads. The wellhead has monitors for pressure and in some cases also temperature. The well is connected to the subsea manifold by a 5 inch

flexible pipe with a typical length of 110 m. The flow lines are insulated by thermoplastic and the heat transfer coefficient is 5.6 W/m^2K. The flow lines are submerged into an approximately 1 m deep ditch. The valves are controlled by HP (high pressure) and LP (low pressure) hydraulic system located topside at Gullfaks C.

1.4.2 Subsea manifold

The flow lines from the wells are connected at the subsea manifold, which is a 10 inch U-shaped pipe. The manifold has horizontal connections for the A and B production pipelines, water injection pipeline, control/umbilical lines from Gullfaks C, control line to the satellite wells and templates and flow lines from wells. The manifold is protected by a structure with the outer measures of 25.6 x 21.2 x 6 m. The design pressure and temperature for the subsea equipment is 5000 Psi (345 bar) and 80 degrees C. The water depth at the subsea manifold is 200 m. The new PLIM was installed in 2006 and replaced the subsea manifold.

1.4.3 Production pipelines

The production pipelines are 10 inch low alloyed carbon steel with 0.5 % chromium, and flexible pipes the last 300 m before the subsea manifold [14]. To achieve a heat transfer coefficient of 5.6 W/m^2K, the pipelines are placed in 0.9 m deep ditches and covered by epoxy and polypropylene. Where the pipelines are uncovered, a thermal protection layer of polypropylene foam is added. The risers have no thermal insulation, only an epoxy and polypropylene protection layer. The pipelines are equipped with sacrificial anodes for corrosion protection. Internal inspection and clean-up of pipelines are done by pigging from Gullfaks C.

2 LITERATURE REVIEW

Flow assurance is an important part of pipeline technology for subsea oil and gas production. Flow assurance addresses all issues in the reliable, manageable and economical transport of the fluid to a processing plant [5]. Low temperatures and high hydrostatic pressure creates major challenges to design and operation of pipelines and other subsea equipment. Low fluid temperature is caused by three main reasons [5]; shallow reservoirs, long tie-back distance and large adiabatic pressure drop. The temperatures in the flowline should be kept above wax deposition temperature during steady-state production and above the HET (hydrate equilibrium temperature) during start-up and cool-down periods. In case of unplanned production shutdown, it is of large importance that operating procedures covers all scenarios so that hydrate formation is avoided. Subsea pipelines and equipment are usually equipped with passive thermal insulation and in steady state conditions this is enough to maintain the desired temperature. To achieve acceptable temperature conditions during start-up or shut-down, a system for active heating can be used. Active heating by use of pipe bundle with a circulating hot fluid or direct electrical heating is used in different Statoil production systems, such as the Gullfaks and Åsgard fields. Figure 2-1 show a bundle pipe with hot water as active heating. The carrier pipe is filled with N_2 and the sleeve pipe is filled with water to ensure a uniform heat distribution.

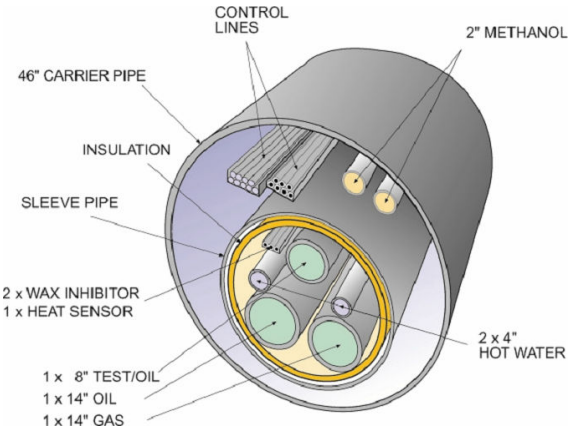

Figure 2-1: Bundle with production pipes, heating and control lines [14]

2.1 Heat transfer equations

A subsea pipeline can be treated as a heat exchanger with the coolant outside the pipe. Subsea pipelines is usually a multi-layer pipe, a steel pipe of stainless steel quality, a layer of corrosion protection (coating) and an insulation material, typically polypropylene. In some cases the pipeline also gets a layer of gravel on top, for trawl protection.

The general heat transfer equations are:

$$q = U \cdot A \cdot \Delta T_{LM} \qquad (2\text{-}1)$$

Fourier's law:

$$q = -k \cdot A \cdot \frac{\partial T}{\partial x} \qquad (2\text{-}2)$$

To describe the heat transfer system in the stagnant zone of the deadleg, a one-dimensional model has been developed, see Figure 2-2

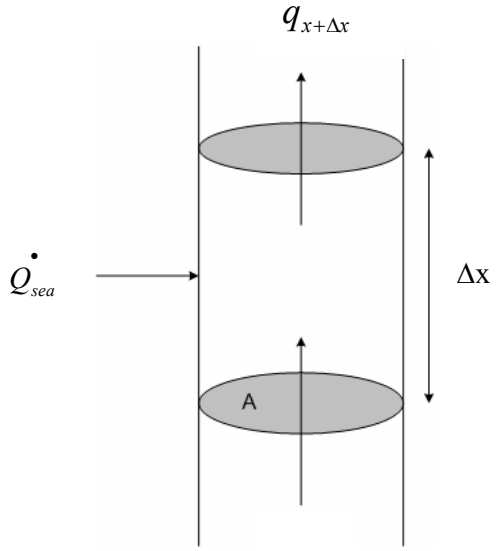

Figure 2-2: Heat transfer system

The general heat transfer model

$$\frac{dU_i}{dt} = \dot{H}_{in} - \dot{H}_{out} + \dot{Q} - W \qquad (2\text{-}3)$$

Where

$\frac{dU_i}{dt} = 0$, stationary system

$\dot{H}_{in} = 0$

$\dot{H}_{out} = 0$

$$-W = 0$$

$$\Rightarrow \dot{Q} = \left(q''_x - q''_{x+\Delta x}\right)\cdot A + \dot{Q}_{sea} \qquad (2\text{-}4)$$

$$q''_x = -k\frac{dT}{dx} \qquad (2\text{-}5)$$

$$\dot{Q}_{sea} = U \cdot S \cdot \left(T_{gas} - T_{sea}\right) \qquad (2\text{-}6)$$

U is the thermal resistance.

Where the surface area S is

$$S = c \cdot \Delta x \qquad (2\text{-}7)$$

and c= pipe outer circumference

Combining equations (*2-4)* and *(2-6)* gives

$$0 = \left(q''_x - q''_{x+\Delta x}\right)\cdot A + U \cdot c \cdot \Delta x \cdot \left(T_{gas} - T_{sea}\right) \qquad (2\text{-}8)$$

Dividing all terms with Δx

$$\frac{-\left(q''_x - q''_{x+\Delta x}\right)}{\Delta x}\cdot A = U \cdot c \cdot \left(T_{gas} - T_{sea}\right) \qquad (2\text{-}9)$$

The left hand side term is the derivative of q''

$$\Rightarrow A\left(-\frac{dq}{dx}\right) = c \cdot U\left(T_{gas} - T_{sea}\right) \qquad (2\text{-}10)$$

Inserting equation *(2-5)*

$$A\left(-\frac{d}{dx}\right)\left(-k\frac{dT}{dx}\right) = c \cdot U \cdot \left(T_{gas} - T_{sea}\right)$$

Assumes that $\frac{dk}{dx} = 0$

$$k \cdot A\frac{d^2}{dx^2}(T) = c \cdot U \cdot \left(T_{gas} - T_{sea}\right) \qquad (2\text{-}11)$$

Assumes that T_{sea}=*constant*

$$k \cdot A\frac{d^2}{dx^2}\left(T_{gas} - T_{sea}\right) = c \cdot U \cdot \left(T_{gas} - T_{sea}\right)$$

$$\left(T_{gas} - T_{sea}\right) = \sigma$$

Replacing $\left(T_{gas} - T_{sea}\right)$ with σ

$$k \cdot A \frac{d^2}{dx^2} \cdot \sigma = c \cdot U \cdot \sigma$$

The heat transfer model is

$$\underline{\underline{\frac{d^2\sigma}{dx^2} = \frac{c \cdot U \cdot \sigma}{k \cdot A}}} \qquad (2\text{-}12)$$

2.2 External flow

According to [1] heat transfer to or from a surface is classified as external flow where boundary layers develop without constraints due to adjacent surfaces. In the flow region outside of the boundary layer gradients of velocity, temperature and concentration can be considered as negligible. For the subsea pipe, the heat transfer occurs under forced convection conditions. The velocity in the seawater are low, in the range of 0.1 to 2 m/s [10]. Figure 2-3 shows a velocity normal to the cross-section of the pipe, where V is the free stream velocity [1], D is the diameter, θ is the angle from the stagnation point and $u_\infty(x)$ is the streamline velocity.

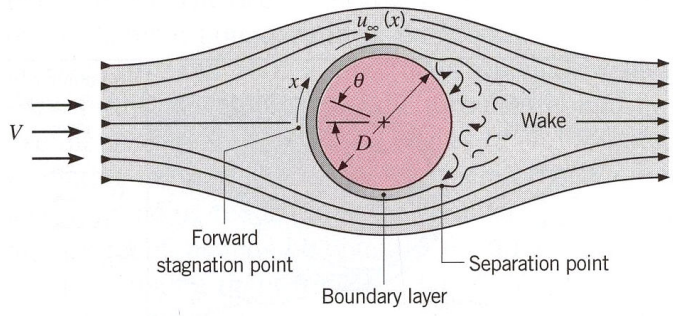

Figure 2-3: Boundary layer formation and separation on a circular cylinder in cross flow [1]

The convection coefficients must be determined for the different flow geometries. The Nusselt number is a dimensionless temperature gradient at the surface and may be expressed by the following correlations [1]:

$Nu_x = f(x^*, \mathrm{Re}, \mathrm{Pr})$ or

$\overline{Nu_x} = f(\mathrm{Re}_x, \mathrm{Pr})$

Where x is a particular point at the surface and the overbar is the average from x*=0, where the boundary layer starts to develop.

The Reynolds number is defined as

$$\mathrm{Re}_D = \frac{\rho V D}{\mu} = \frac{V D}{\nu} \qquad (2\text{-}13)$$

The characteristic length D is the outer diameter of the pipe. If $\mathrm{Re}_D \le 2 \cdot 10^5$ the boundary layer is in the laminar area and separation is likely to occur at θ≈80°. When $\mathrm{Re}_D \ge 2 \cdot 10^5$, boundary layer transition occurs, and separation starts at θ≈140°. Figure 2-4 shows the laminar boundary layer separation. The heat transfer in the separation zone will be lower and the coldest point will be in frontal part of the pipe.

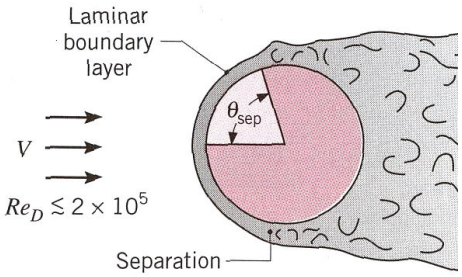

Figure 2-4: The effect of turbulence on separation [1]

The Prandtl number is the ratio of the momentum and thermal diffusivities and is defined as

$$\mathrm{Pr} = \frac{c_p \mu}{k} = \frac{\nu}{\alpha}, \text{ where } \alpha \text{ is the thermal diffusivity.} \qquad (2\text{-}14)$$

The convection heat transfer coefficient *h* can be calculated from Nusselts number

$$\overline{Nu}_D = \frac{\bar{h} D}{k} = C\,\mathrm{Re}_D^m\,\mathrm{Pr}^{\frac{1}{3}} \qquad (2\text{-}15)$$

The constants C and m can be found in Table 2-1.

Table 2-1: Constants of equation for the circular cylinder in cross flow [1]

Re_D	C	m
0.4-4	0.989	0.330
4-40	0.911	0.385
40-4000	0.683	0.466
4000-40,000	0.193	0.618
40,000-400,000	0.027	0.805

2.3 Hydrates

Hydrates are a well-known problem in the oil production and processing systems. Hydrates form under given conditions, such as low temperature, high pressure and water present in the system. Subsea pipelines and equipment are vulnerable because of the low temperature, also in tropical areas. The gas present in the well-stream contains a various amount of gas which is saturated with vaporized water. Water collects in the low-points of the pipeline and hydrate can be formed as a solid block or slurry. The ratio between water and gas can be as in Figure 2-5.

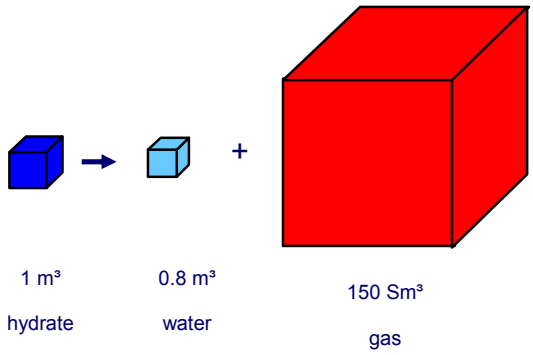

Figure 2-5: Water-Gas ratio in hydrates [14]

Hydrate deposition at the inner wall of the pipe may cause partial or total plugging resulting in reduced gas flow [3]. Although often encountered in practice, this phenomena still is poorly understood and several unanswered questions. Engineers can predict in which part of the pipeline hydrates will form by calculations, but the hydrate formation rate can be hard to predict adequately. Small molecules of non-polar gases such as hydrocarbons form hydrate together with water. This is a physical bond, not chemical and they have different structures. The mass ratio is 85% water and 15% gas [4].

2.3.1 Hydrate control

To avoid hydrates from deposit inside a pipeline, the HET (hydrate equilibrium temperature) is an important parameter. To determine this temperature a hydrate equilibrium curve is used, see Figure 2-6. This is empirical curves related to pressure and temperature, and can be calculated in thermo-dynamical applications, e.g. Hysys. To avoid hydrate formation operation conditions must be kept below the hydrate equilibrium curve. The curves can be moved to the left by adding a thermo dynamical inhibitor, e.g. MEG (mono ethylene glycol) or methanol. The different curves in Figure 2-6 shows the effect of adding a certain weight percent of inhibitor to the system. A rule of thumb is that the HET is about 20 degrees Celsius.

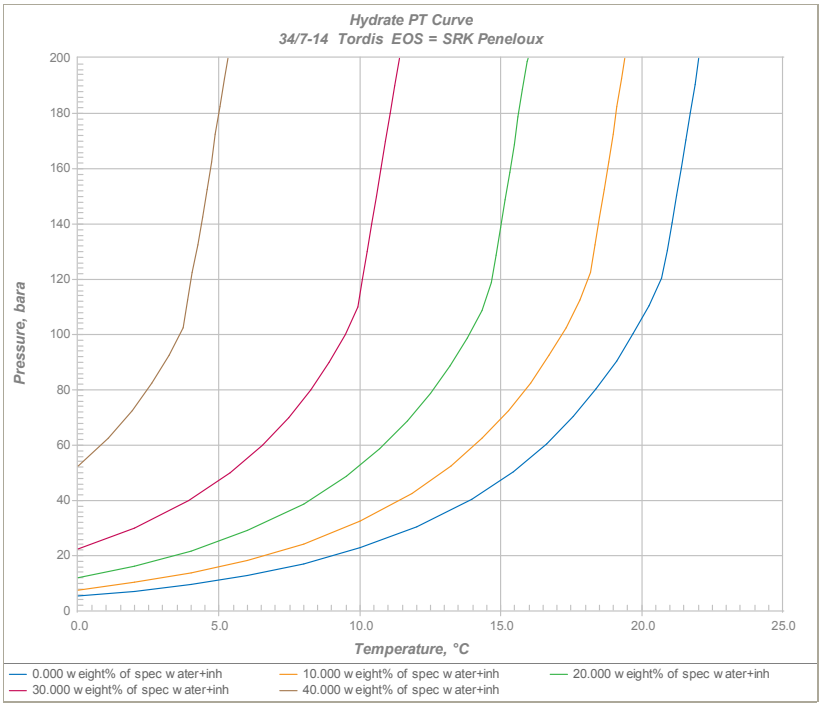

Figure 2-6: Hydrate equilibrium curve for the Tordis field [14]

Hydrate control can be divided into different practices [14]:

- Hydraulic. Replacement of fluid by circulating the pipeline with e.g. stabilized crude oil. Gas injection in pipeline to avoid water to collect in low spots. Depressurization of pipeline to stay out of hydrate formation area. Pressurization; rapidly start-up where a well with high fraction of gas heats the pipeline with heat of compression.
- Heating of pipeline by use of insulation, direct electric heating or bundles where a heating medium circulates continuously and heat tracing.
- Chemical inhibition by injection of methanol, glycols, low concentrate inhibitors, salts.
- Removal of water by gas dehydration and reduction of water cut. This can be done by optimize production parameters and closing off water production zones by well intervention.
- Production without special actions; production is always above HET

2.3.2 Removal of hydrate plugs

If a hydrate problem occurs, the effects can be minor production shutdown or in worst case; a plug that is impossible to remove and huge economical consequences. Therefore, hydrate

remediation must be addressed early in the design phase as a part of the hydrate control philosophy [14].

Hydrate remediation methods may be organized into groups of:

- Chemical methods
- Heating
- Depressurization
- Mechanical methods

Chemical methods

Addition of inhibitor will reduce the melting temperature and the hydrate equilibrium curve will be moved to the left. Insufficient contact between inhibitor and plug may stop the melting process. Water is released in the initial phase of melting and a water film prevents contact between inhibitor and plug. There is a large variation in plug properties and melting efficiency. This can be due to difficulties of predicting plug properties and varying melting efficiency for plugs.

Heating

Melting of hydrate by heating the pipe from the outside. This has to be done carefully and gas has to be led away to safe location to avoid pressure build up avoid new hydrate problems. An accurate position of plug is needed to make sure that heating starts at the end of the plug.

Depressurization

Depressurizing can be done by lowering the pressure below the hydrate equilibrium curve on one or both sides of the plug. The plug will start to melt. This is not without risk, melting starts at the wall and the plug can start to move with high velocity. A plug without control can be dangerous to both equipment and people.

Mechanical methods

Hydrate plugs can be removed by different mechanical devices, by the use of tractor and pigging technology. They can be launched both topside and subsea. They can reach up to 15 km and pass 90° bends and have pull force up to 30 ton. Figure 2-57 shows a tractor which turns the crystals into dispersion by high pressure jetting.

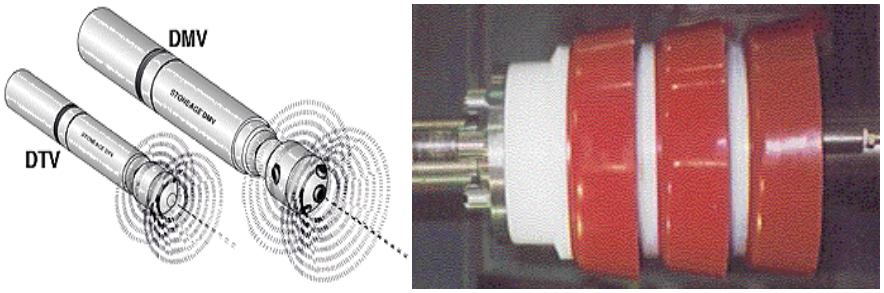

Figure 2-7: Tractor for removal of hydrate and clean-up pig [14]

2.4 Modeling heat transfer in Fluent

There are three main methods for heat transfer; by conduction, convection and radiation [13]. The physical models of conduction and/or convection are the simplest, while buoyancy driven flow, natural convection and radiation models are more complex. Fluent solves a variation of the energy equation in the defined case.

2.4.1 Convective and conductive heat transfer in Fluent

Heat transfer can be included in both the fluid and the solid parts of the model. The range of problems that can be handled by Fluent is wide, from thermal mixing to conduction in a composite solid [13]. The energy equation solved by Fluent is written in the following form

$$\frac{\partial}{\partial t}(\rho E) + \nabla \cdot (\vec{v}(\rho E + p)) = \nabla \cdot \left(k_{eff} \nabla T - \sum_j h_j \vec{J}_j + (\bar{\bar{\tau}}_{eff} \cdot \vec{v}) \right) + S_h \qquad (2\text{-}16)$$

Where k_{eff} is the effective conductivity, $k + k_t$, where k_t is represents the turbulent thermal conductivity defined according to the chosen turbulence model. $\vec{J}_j$ is the flux of diffusion of species j. At the right hand side of the equation, the first terms represents the energy transfer due to conduction, species diffusion and viscous dissipation. The source term S_h includes heat of reaction and other defined volumetric heat sources. The energy term E is defined as

$$E = h - \frac{p}{\rho} + \frac{v^2}{2} \qquad (2\text{-}17)$$

Where the enthalpy h is defined for ideal gases as

$$h = \sum_j Y_j h_j \qquad (2\text{-}18)$$

For incompressible flow

$$h = \sum_j Y_j h_j + \frac{p}{\rho} \qquad (2\text{-}19)$$

Y_j is the mass fraction of species j and

$$h_j = \int_{T_{ref}}^{T} c_{p,j} dT \qquad (2\text{-}20)$$

Where T_{ref} is 298.15 K

2.5 Buoyancy

In a vertical deadleg both free and forced convection phenomena will be present. Forced convection is driven by the velocity/momentum of the flow in the main pipe. At a certain distance from the main pipe forced convection is no longer present. In this part of the deadleg free convection driven by buoyancy forces will contribute to circulation of the fluid inside the pipe. The fluid will move upward in the center of the pipe. As the fluid in the zone close to the wall will cool down, a downwards movement will occur. The buoyancy force is due to gravity and density gradients as a result of temperature gradients [1]. Due to gravity, it is assumed that free convection will not influence significant on the flow pattern in a horizontal deadleg. To investigate the importance of buoyancy, a CFD simulation of a closed cylinder has been performed.

2.5.1 Rayleigh number

The Rayleigh number can determine if the boundary layer is in the turbulent or laminar area. According to [13], Rayleigh numbers less than 10^8 indicates a buoyancy-induced laminar flow and transition to turbulence occurring over the range of $10^8 < Ra < 10^{10}$. The Rayleigh number is calculated by equation (2-21)

$$Ra = \frac{L^3 \cdot \rho^2 \cdot g \cdot \beta \cdot \Delta T \cdot C_p}{\mu \cdot k} \qquad (2\text{-}21)$$

Table 2-2: Symbols used in equation (2-21)

β	coefficient of expansion
Cp	heat capacity
ΔT	temperature difference
g	gravity acceleration
k	thermal conductivity
L	characteristic length
μ	viscosity
ρ	density

3 CFD SIMULATION SETUP

3.1 Developing the geometry

The geometries where developed in Gambit 2.3.16, a tool for drawing and generation of mesh. The base geometry is a straight pipe with a 90^o branch attached. The length of the straight pipe is $20D_i$, this is to ensure a fully developed flow before the branch. The length of the branch is $10D_i$ from the center of the main pipe, and the pipe section downstream of the branch has the length of $3D_i$. Based on the former work done by Habib [7, 9, 16] and IFE [10] and also initial simulations in this project, who indicates flow into 3-4 D into the branch, the length of the branch was set to be $10D_i$. Figure 3-1 gives an overview of the geometry.

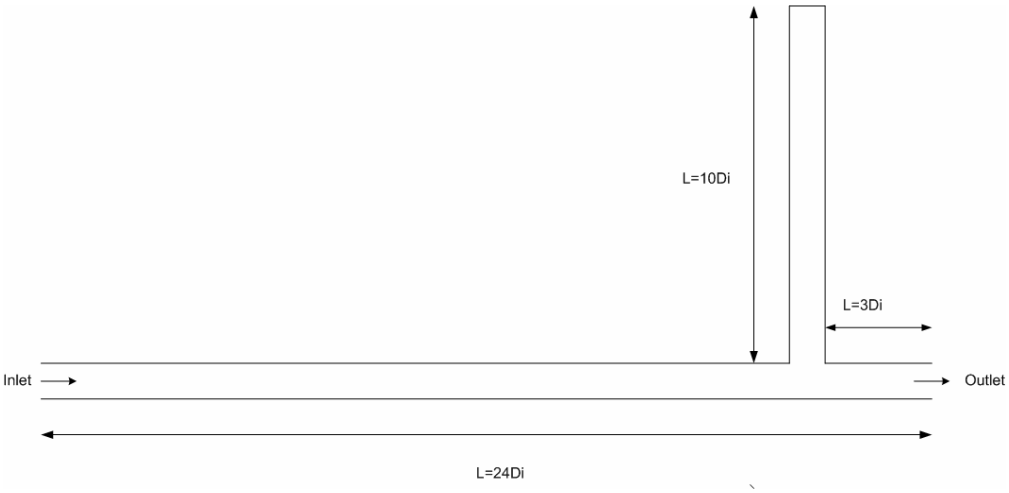

Figure 3-1: Geometry of pipe with branch

The specifications for the 10 inch pipe are given in the piping class sheet GD251A CL2500 [15]. See Table 3-1.

Table 3-1: Pipe size and wall thickness

Nominal size [in]	10
Outer diameter [mm]	273.1
Wall thickness [mm]	25.44

3.1.1 The deadleg

The deadleg was created Gambit in by connecting a horizontal and vertical cylinder, representing the main pipe and the deadleg. Two additional cylinders form a volume on the outside to

represent the steel part of the pipe. The two volumes were divided into smaller volume-sections to avoid skewness in the mesh and be able to fit the size of the cells. The intersection and the deadleg, is provided with a fine mesh. This is the part of the system where heat transfer occurs. The straight section has more coarse mesh, since the purpose of this part is to develop the flow. A structured mesh is applied to make convergence easier [6]. Figure 3-2 shows the mesh at the outer surface of the pipe.

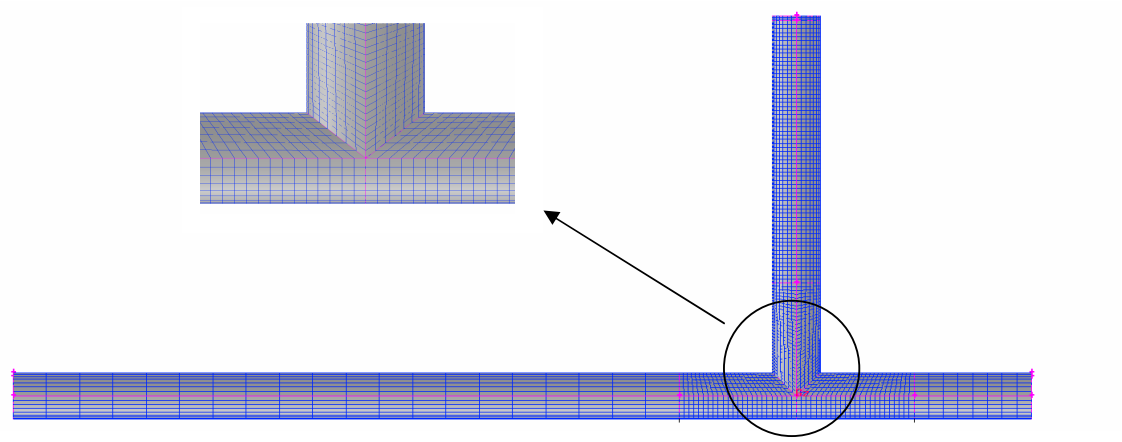

Figure 3-2: Pipe and branch with mesh

A boundary layer was attached to the inner wall of the pipe. This was to ensure a wall y^+ within the recommended range for high Reynolds number. The center section of the pipe has triangular mesh, see Figure 3-3. The three outer rows represent the steel wall. The boundary layer in the fluid zone grows towards the center of the pipe.

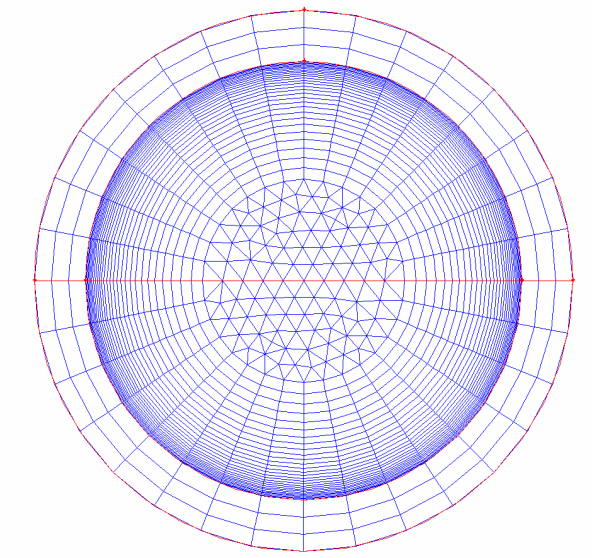

Figure 3-3: Cross section mesh

In practice there will be a valve at the end of the branch. When the valve is closed, the branch will act as a deadleg. The valve is usually un-insulated, and the geometry is complex and difficult to model. To simplify the modeling of the valve, a steel plate is placed at the end of the branch. The plate has the same thickness as the rest of the steel walls, see Figure 3-4.

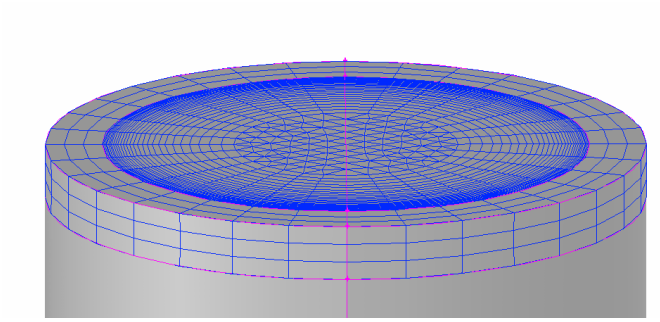

Figure 3-4: Simplified model of valve with mesh

The boundaries and continuum types specified in Gambit, and where set as in Table 3-2.

Table 3-2: Boundaries and continuum

Boundaries		
Inlet	Mass flow inlet	
Outlet	Pressure outlet	
Walls	Outside wall	Branch
		Pipe
		Valve
Continuum		
Fluid volume	Fluid	
Walls	Steel	
Valve	Steel	

The mesh contains

- 204024 cells
- 606128 faces
- 197894 nodes

3.2 Simulation of the deadleg

The simulations are preformed in Fluent 6.2.16. The mesh described in 3.1.1 is the basis for all simulations. The main purpose for the simulations is to examine temperature profile in an un-insolated deadleg and the flow pattern inside the deadleg. Both vertical and horizontal deadlegs are simulated by changing the direction of gravity in Fluent. The equation of state for the gas in Fluent is non-compressible ideal-gas.

The base case is natural gas under the following conditions

- Pressure 100 bar (10^7 Pa)
- Temperature 65 ^{o}C (338 K)
- Velocities of $\approx$2 and $\approx$9 m/s
- Sea water temperature of 7 ^{o}C

All properties of gas are given in appendix C are actual test data from the Skinfaks/Rimfaks field. Two different heat transfer coefficients (HTC) are applied to examine the sensitivity of the heat transfer number.

3.2.1 Boundary conditions

Outside wall

Convective heat transfer coefficient is set at outer wall. The HTC of 580 W/m^2 K relates to a velocity in the surrounding sea water of 0.2 m/s. Another HTC of 1100 W/m^2 K relates to a sea water velocity of 0.5 m/s. The HTC's are calculated based on data from Statoils department of Metocean, Mapping and Geotechnics [12] and the sea water properties collected from [11]. If the seawater velocity is assumed to be 0.5 m/s, D is 0.273 m, and the viscosity ν is $1.59 \cdot 10^{-6}$ m^2/s [11], the Reynolds number is

$$\mathrm{Re}_1 = \frac{0.5 m s^{-1} \cdot 0.273 m}{1.59 \cdot 10^{-6} m^2 s^{-1}} = \underline{85850} \quad \textit{(2-13)}$$

For a 10 inch pipe with a 30 mm insulation layer, the Reynolds number is

$$\mathrm{Re}_2 = \frac{0.5 m s^{-1} \cdot 0.333 m}{1.59 \cdot 10^{-6} m^2 s^{-1}} = \underline{104717}$$

The Prandtl number *(2-14)*

$$\mathrm{Pr} = \frac{1.59 \cdot 10^{-6} m^2 s^{-1}}{1.37 \cdot 10^{-7} m^2 s^{-1}} = \underline{11.6}$$

The Nusselts numbers for the two cases are *(2-15)*

$$\overline{Nu_1} = 0.027 \cdot 85850^{0.805} \cdot 11.6^{1/3} = \underline{572.6}$$

$$\overline{Nu_1} = 0.027 \cdot 104717^{0.805} \cdot 11.6^{1/3} = \underline{671.9}$$

Equation (2-15) solved for *h* gives the following results

$$\bar{h}_1 = \frac{\overline{Nu_D} \cdot k}{D} = \frac{572.6 \cdot 0.57 W m^{-1} K^{-1}}{0.273 m} = \underline{\underline{1195 W m^{-2} K^{-1}}}$$

$$\bar{h}_1 = \frac{\overline{Nu_D \cdot k}}{D} = \frac{671.9 \cdot 0.57 Wm^{-1}K^{-1}}{0.333m} = \underline{\underline{1150 Wm^{-2}K^{-1}}}$$

Assuming a sea water velocity of 0.2 m/s, the heat transfer coefficient will be roughly 580 W/m^{2}K.

Valve

The same as for the outside wall.

Inlet

The inlet is defined as a mass flow inlet, with 6 and 26 kg/s as the mass flow. This corresponds to ca. 2.2 m/s and 9 m/s. The choice of velocities is based on earlier simulations done by IFE [10] and assumptions made by the student.

Outlet

The outlet is defined as a pressure outlet.

For more details se appendix B and C

3.2.2 Turbulence model

The turbulence model used in all deadleg simulations is the k-ε model, with standard wall functions. This is a turbulent flow regime, and the Reynolds numbers for the two velocities are

$$\mathrm{Re} = \frac{\rho \cdot u \cdot D}{\mu} = \frac{88.6 kg/m^3 \cdot 2.2 m/s \cdot 0.222 m}{1.56 \cdot 10^{-5} kg/m \cdot s} = \underline{2.7739 \cdot 10^6}$$

$$\mathrm{Re} = \frac{\rho \cdot u \cdot D}{\mu} = \frac{88.6 kg/m^3 \cdot 9 m/s \cdot 0.222 m}{1.56 \cdot 10^{-5} kg/m \cdot s} = \underline{1.1348 \cdot 10^7}$$

This is within the recommended range for the k-ε turbulence model [8].

3.2.3 Residuals

All simulations are converged by a residual value of 10^{-5}. In addition, monitors where set up evaluate convergence.

4 RESULTS

The results are presented in this chapter. One of the main objectives in this project is to evaluate the length of the circulating vortices driven by the flow in the main pipe. Temperature profiles and velocity are the parameters that are in focus in this chapter. For the vertical deadleg, the effect of buoyancy will influence on the flow field, and the simulation setup and results are presented in chapter 4.9.

Table 4-1 gives an overview of the simulation cases.

Table 4-1: Overview of simulation cases

Case	***Orientation***	***Mass flow [kg/s]***	***Velocity [m/s]***	***HTC [W/m^{2}K]***
1a	Vertical	6	2.2	580
1b	Vertical	6	2.2	1100
2a	Horizontal	6	2.2	580
2b	Horizontal	6	2.2	1100
3a	Vertical	26	9	580
3b	Vertical	26	9	1100
4a	Horizontal	26	9	580
4b	Horizontal	26	9	1100

To evaluate the temperature profile towards the end of the deadleg the temperature along the deadleg two lines has been created. The first is the centerline plotted in the y-direction, 0.111 m from the center of the main pipe. The second line is at the left hand side (negative x-direction) of the centerline. This is assumed to be the coldest side of the pipe. The distance from the pipe wall is five mm, see Figure 4-1. This is referred to as wall-line in the figures. The HET is assumed to be approximately 20^{o}C (293 K), and this temperature is marked at the plots to show the length of the zone witch has a lower value.

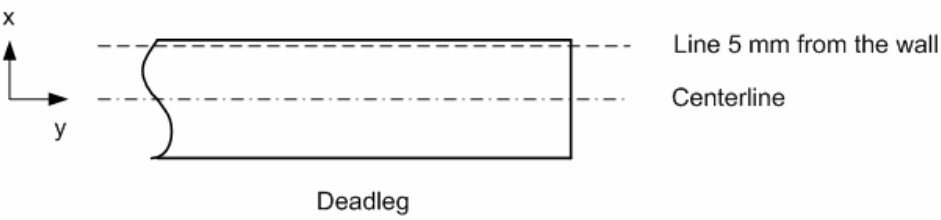

Figure 4-1: Centerline and line five mm from the wall

The cross section planes are as in Figure 4-2 and represents the length of a D_i.

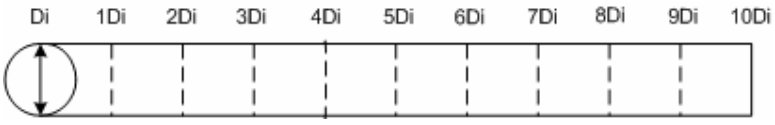

Figure 4-2: Cross section planes in deadleg

4.1 Case 1a, vertical, 2.2 m/s

This is a vertical oriented deadleg. The velocity contours is shown in Figure 4-3. The flow in the main pipe creates a vortex upwards in the deadleg. After a certain distance the velocity will move towards zero.

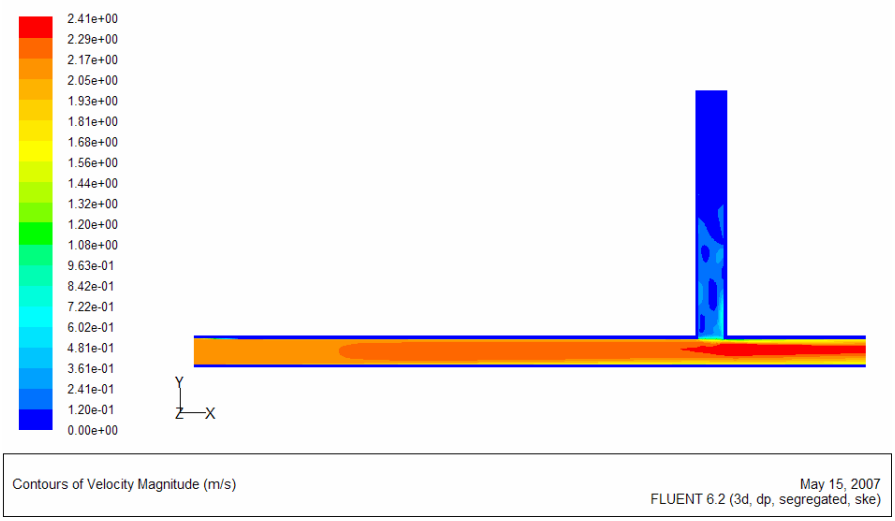

Figure 4-3: Contours of velocity, 2.2 m/s

The low velocity part of the deadleg is shown in Figure 4-4. This is where the velocity is smaller than 0.1 m/s.

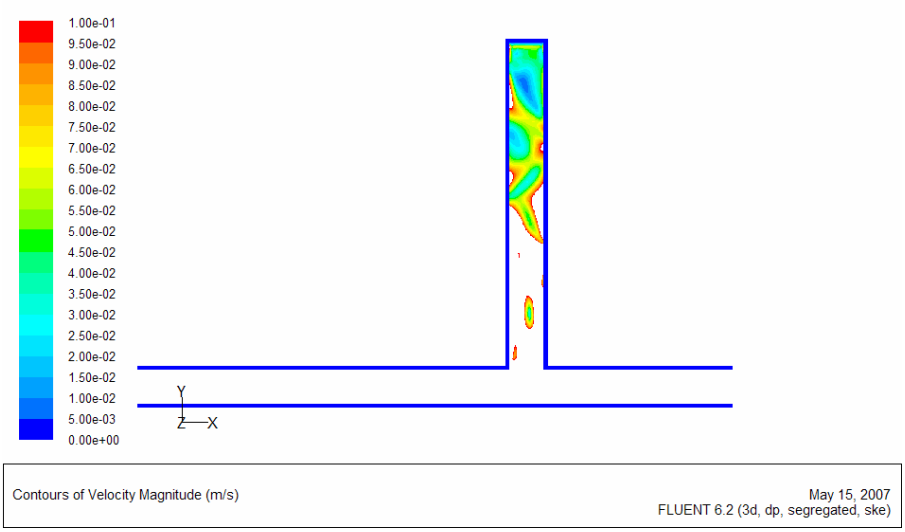

Figure 4-4: Maximum velocity of 0.1 m/s

The temperature decreases towards the end of the deadleg. From Figure 4-5, the temperature in the center of the deadleg is below the HET after a distance of 1.39 m. The average temperature of the centerline is 30°C (303K). The temperature at the end of the centerline is 14°C (287 K).

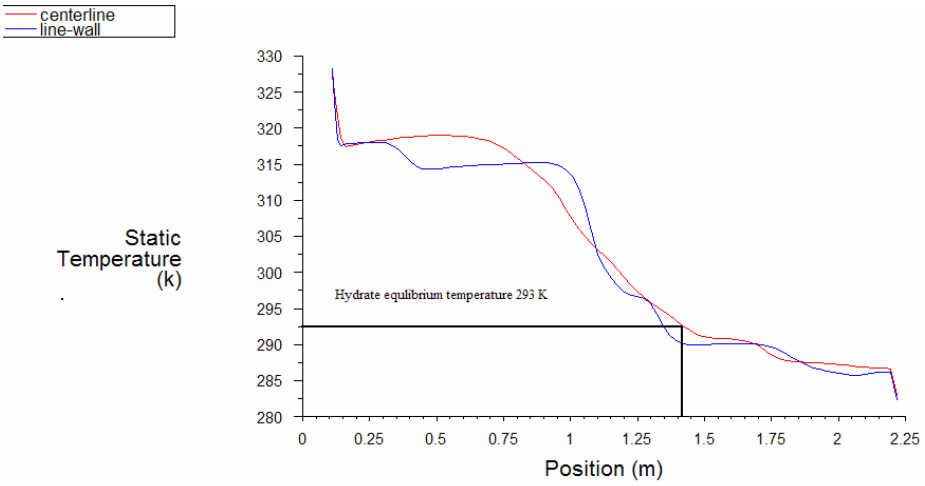

Figure 4-5: Temperature curves

4.2 Case 1b, vertical, 2.2 m/s

This case is similar to 1a except that the HTC is set to 1100. This is equivalent to a sea water velocity of 0.5 m/s. Figure 4-6 shows the temperature outwards in the deadleg. The circular planes represent the length of a D_i. HET is reached after a distance between five and six D_i.

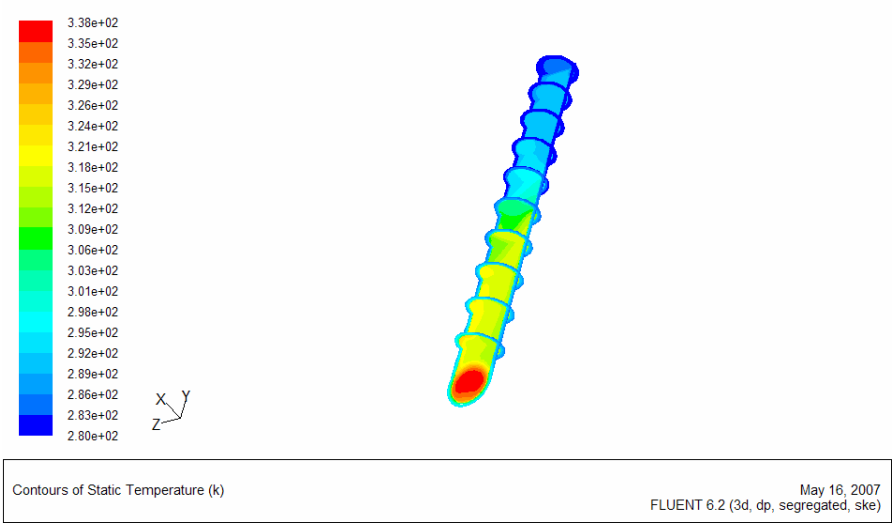

Figure 4-6: Temperature distribution

The HET in the center of the pipe is reached after a distance of approximately 1.42 m into the deadleg. This is shown in Figure 4-7. The surface heat transfer rate of the branch is approximately 1.5 % higher than case 1a. The average temperature of the centerline is 30°C (303K). The temperature at the end of the centerline is 16 °C (289 K).

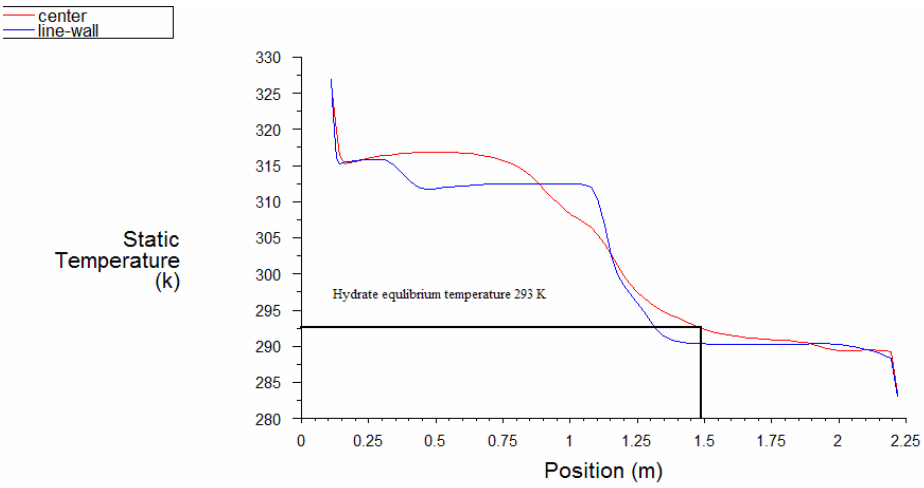

Figure 4-7: Temperature profile in vertical deadleg, h=1100 W/m²K

4.3 Case 2a, horizontal, 2.2 m/s

This is a horizontal oriented deadleg. This simulation is performed with a velocity of 2.2 m/s. Figure 4-8 shows that the temperature is above the HET the whole length of the deadleg. The temperature at the end of the centerline is 38°C (311 K). The average temperature of the centerline is 41°C (314K).

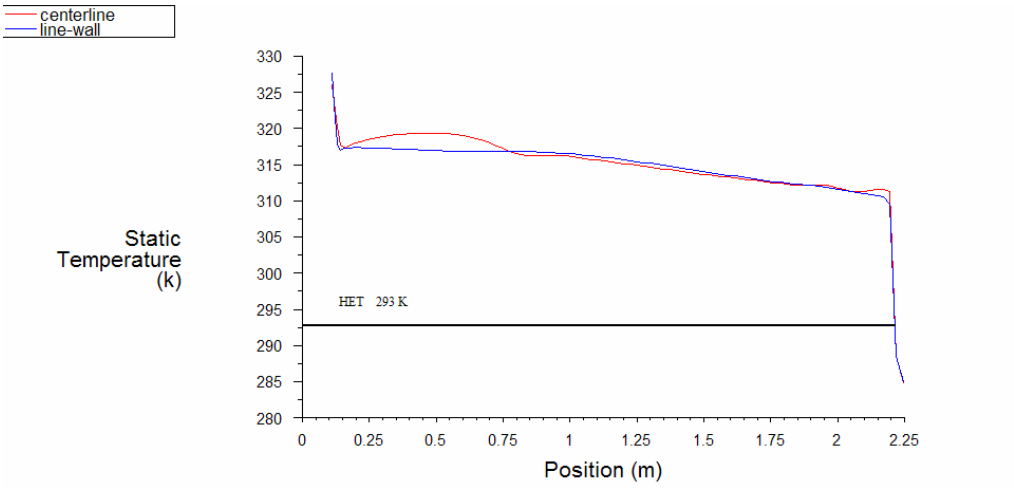

Figure 4-8: Temperature profile in horizontal deadleg, h=580 W/m^{2}K

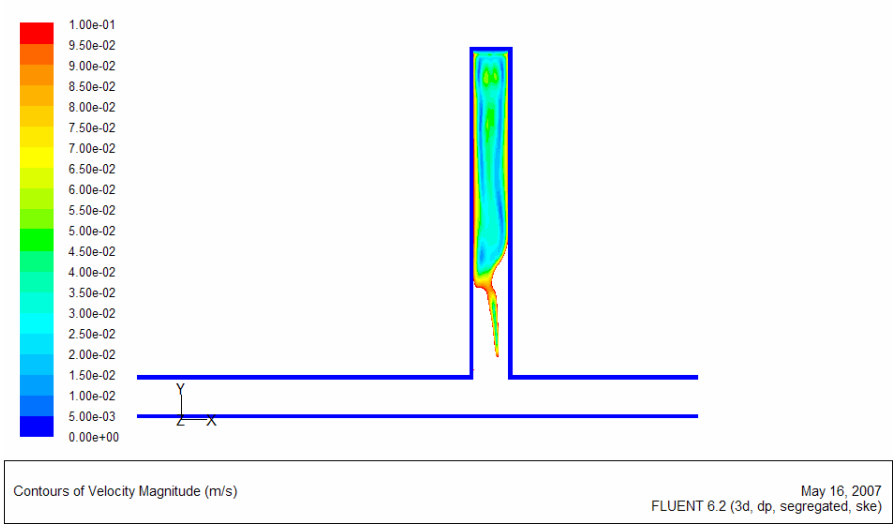

Figure 4-9: Maximum velocity of 0.1 m/s

The horizontal oriented deadleg has a more uniform temperature distribution than the vertical, see Figure 4-10.

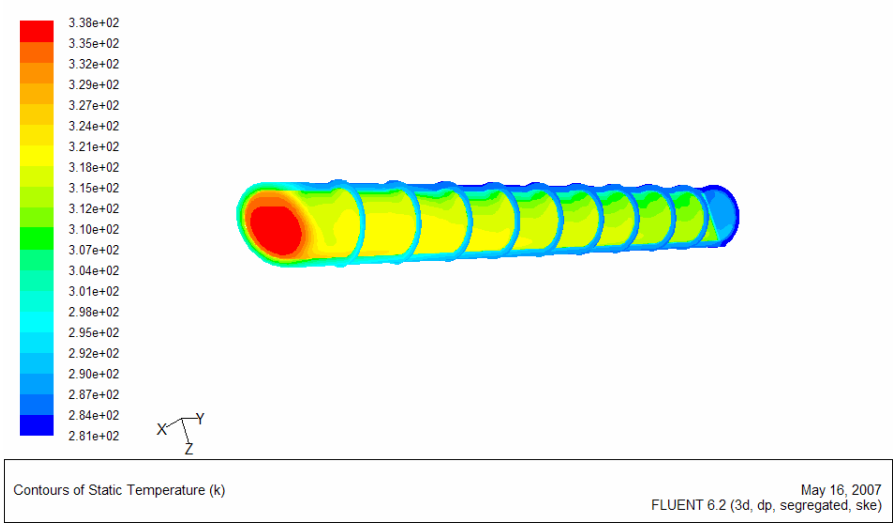

Figure 4-10: Temperature distribution

4.4 Case 2b, horizontal, 2.2 m/s

This case is similar to 2a except that the HTC is set to 1100. Figure 4-11 shows that the temperature is above the HET in the whole length of the deadleg. The surface heat transfer rate of the branch is approximately 9 % higher than case 2a. The average temperature of the centerline is 40.5°C (313.5 K). The temperature at the end of the centerline is 36°C (309 K).

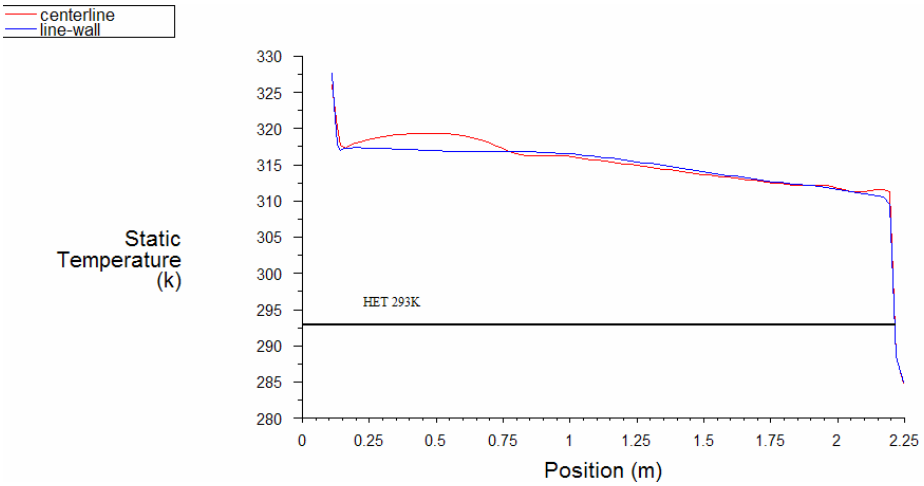

Figure 4-11: Temperature profile in horizontal deadleg, h=1100 W/m²K

Figure 4-12 shows temperature distribution similar to case 2a.

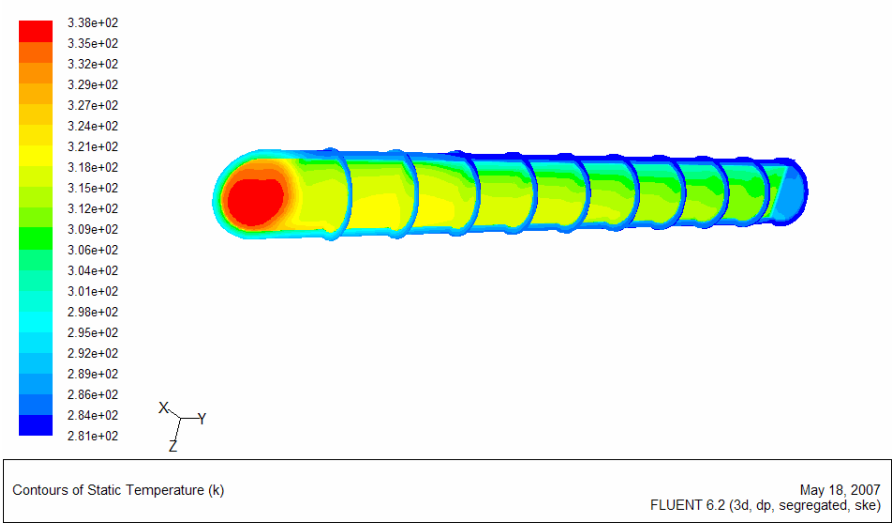

Figure 4-12: Temperature distribution

4.5 Case 3a, vertical, 9 m/s

In this case the velocity is increased to 9 m/s and the orientation is vertical. The HTC is 580 W/m^2K. A higher bulk flow velocity result in higher velocities in the deadleg, and the part of the deadleg with a velocity lower than 0.1 m/s is considerably smaller than the previous cases, see Figure 4-13.

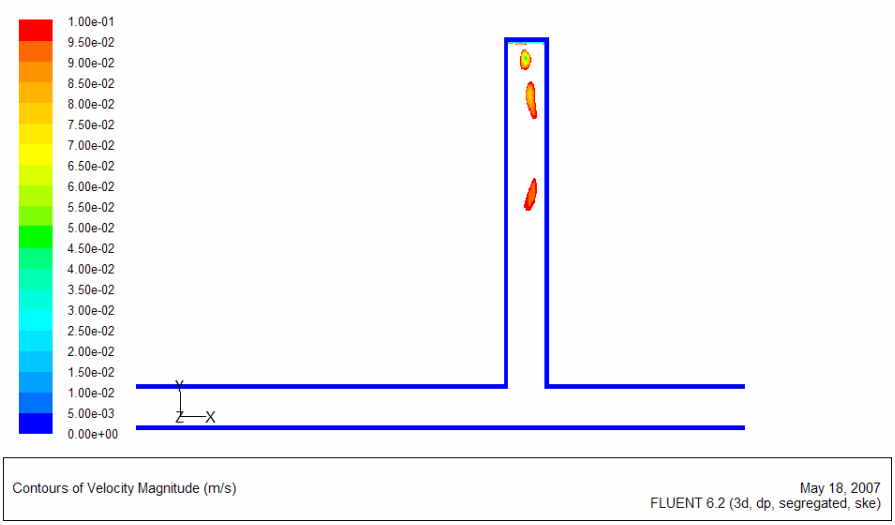

Figure 4-13: Maximum velocity of 0.1 m/s

Figure 4-14 shows that the temperature is above the HET, and the temperature at the end of the centerline is 24°C (297 K). The average temperature of the centerline is 40°C (313 K).

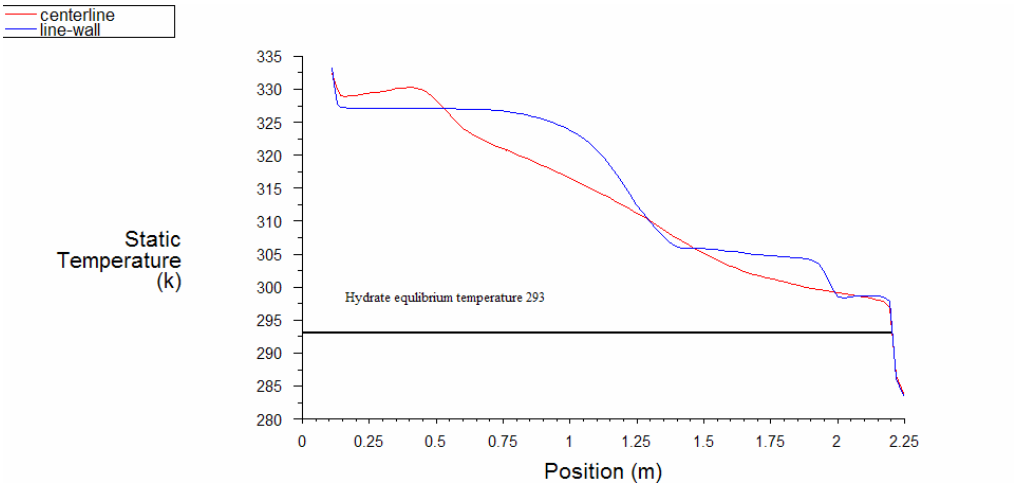

Figure 4-14: Temperature profile in vertical deadleg, h=580 W/m^{2}K

4.6 Case 3b, vertical, 9 m/s

This setup is similar to case 3a with a HTC of 1100 Wm^{-2}K. The HET is reached after 1.51 m and the temperature at the end of the centerline is 12^{o}C (285 K). The average temperature of the centerline is 35 ^{o}C (308 K), see Figure 4-15

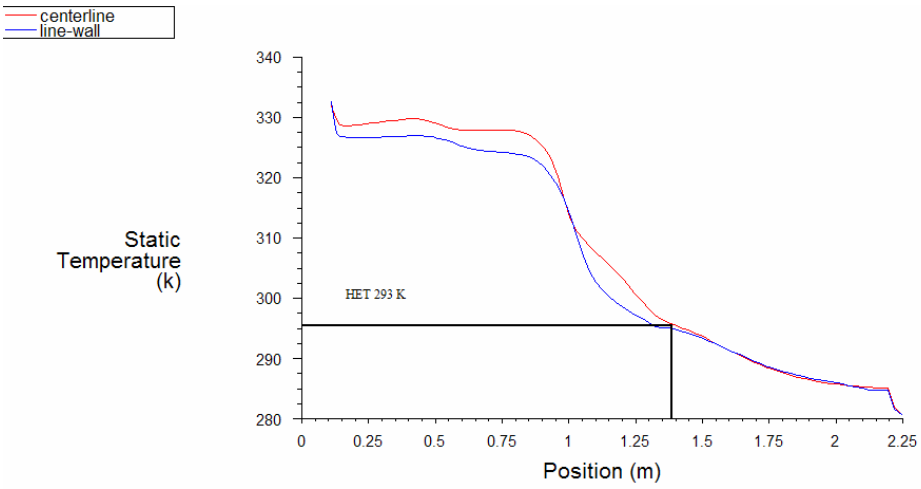

Figure 4-15: Temperature profile in vertical deadleg, h=1100 W/m^{2}K

Figure 4-16 shows the temperature outwards in the deadleg. The circular planes represent the length of a D_i. HET is reached after a distance of approximately six D_i.

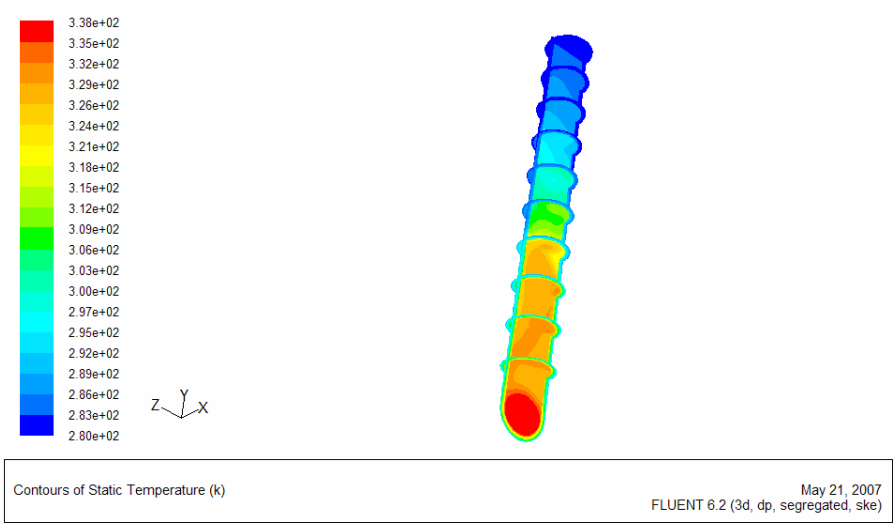

Figure 4-16: Temperature distribution

4.7 Case 4a, horizontal, 9 m/s

In this case the velocity is 9 m/s and the orientation is horizontal. The HTC is 580 W/m^{2}K. Figure 4-17 shows that the temperature is above the HET, and the temperature at the end of the centerline is 44^{o}C (317 K). The average temperature of the centerline is 50^{o}C (323 K).

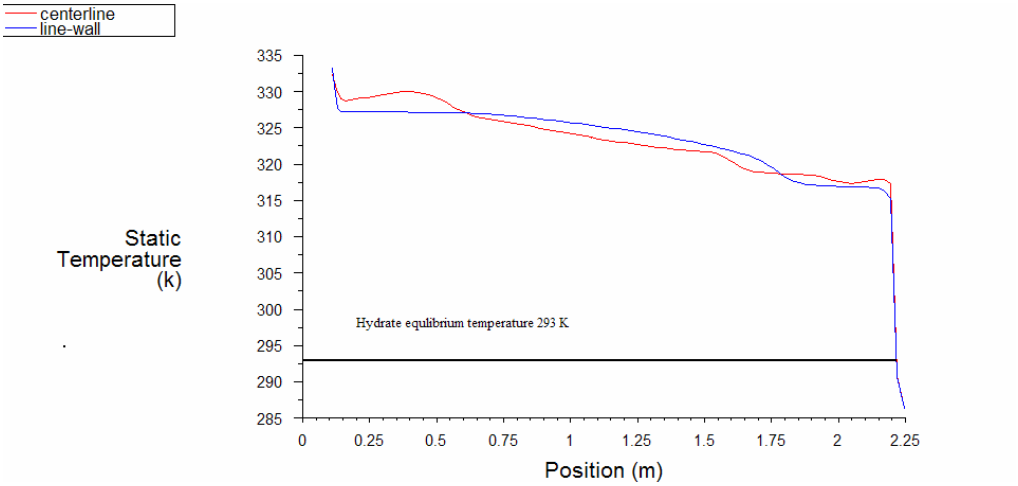

Figure 4-17: Temperature profile in horizontal deadleg, v= 9 m/s

Figure 4-18 shows the temperature distribution in the deadleg. This is more uniform than for the vertical case.

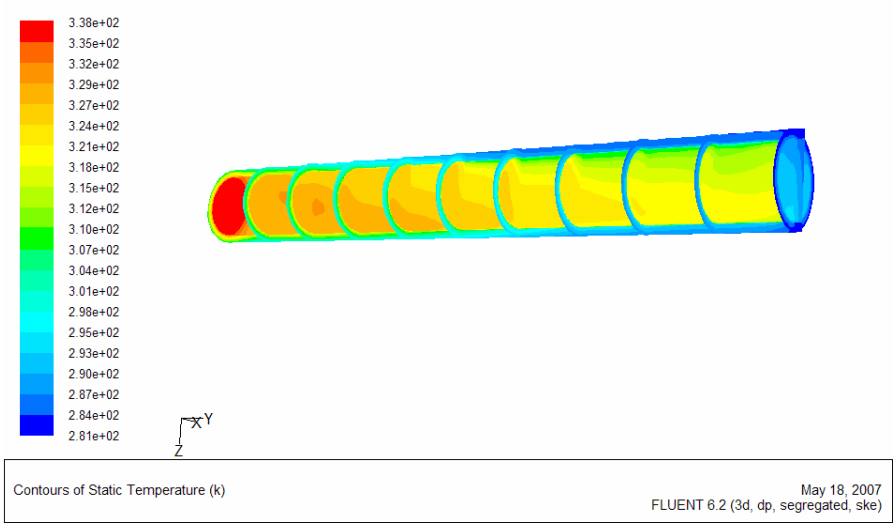

Figure 4-18: Temperature distribution

4.8 Case 4b, horizontal, 9 m/s

This setup is similar to case 4a with a HTC of 1100 $Wm^{-2}K$. The HET is reached after 1.51 m and the temperature at the end of the centerline is 40°C (313 K). The average temperature of the centerline is 48 °C (321 K), see Figure 4-19.

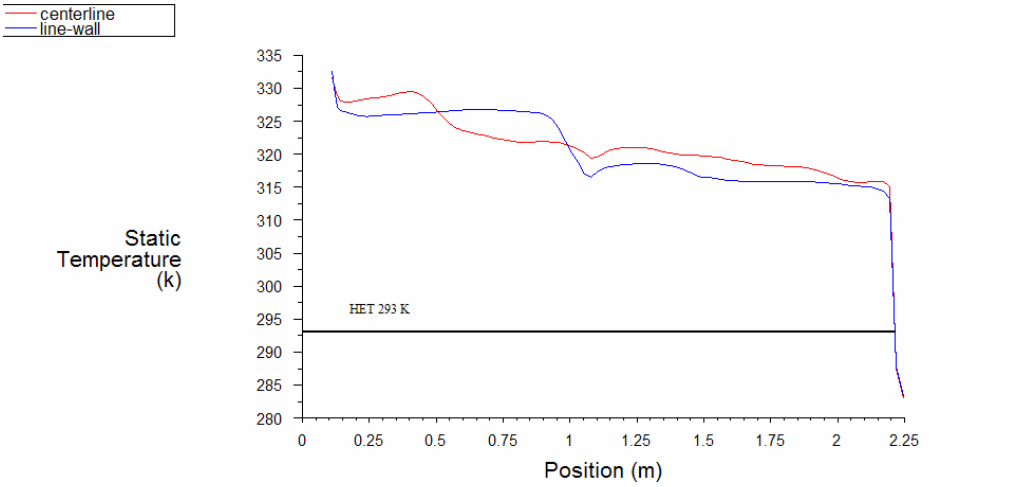

Figure 4-19: Temperature profile in horizontal deadleg, h=1100 W/m²K

4.9 Simulation of buoyancy

The geometry used in this simulation is a vertical closed steel cylinder with a length of 5.5 D_i, see Figure 4-20. The fluid inside is methane and the solid part is steel. The cylinder has a boundary layer and meshed contains 29464 cells, 88236 faces and 29268 nodes. The Rayleigh

number is calculated from equation (4-1) to determine if the boundary layer is in the turbulent or laminar area.

$$Ra = \frac{(1.366m)^3 \cdot (88.6kg/m^3)^2 \cdot 0.00677^oC^{-1} \cdot (65-7^oC) \cdot 2865J/(kg^oC)}{1.56 \cdot 10^{-5} kg/(m \cdot s) \cdot 0.0463W/(m^oC)} = \underline{3.116 \cdot 10^{13}}$$

This gives a Rayleigh number in the turbulent region, even with some insecurity connected to the temperatures used in the calculation. Based on this, the choice of turbulence model for the Bouyancy simulation is RNG k-ε with enhanced wall functions. The boundary conditions are a convective heat transfer coefficient at the outer wall of 580 W/m^2 ºC. The hot end has a constant temperature of 338 K. All material properties and dimensions are equal to the simulations of the deadleg, see appendix B and C for details.

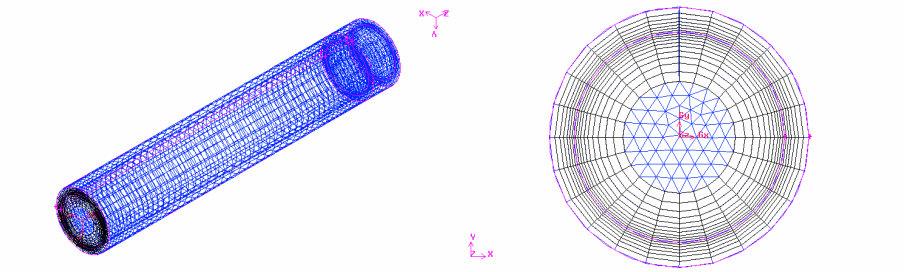

Figure 4-20: Cylinder mesh and cross section

The fluid inside of the cylinder is defined as non-compressible ideal gas. Due to the constant temperature at the end and the cooling effect at the outside wall, an upward vortex is expected in the center part of the cylinder, and a downward movement close to the wall.

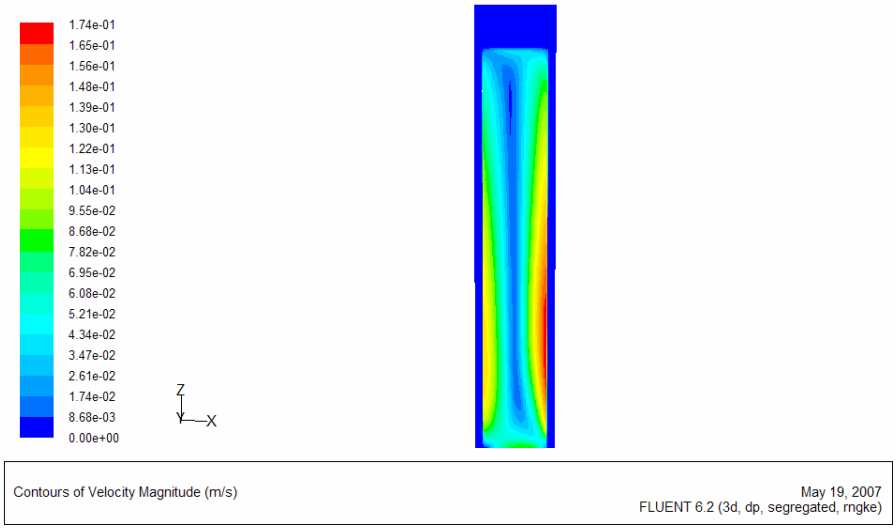

Figure 4-21: Contours of velocity in closed cylinder

Figure 4-21 shows that the highest velocity of 0.17 m/s is close to the wall. In the vector plot in Figure 4-22 the circulating cell driven by the difference in temperature can be seen. The highest velocities are in the z-direction and along the wall.

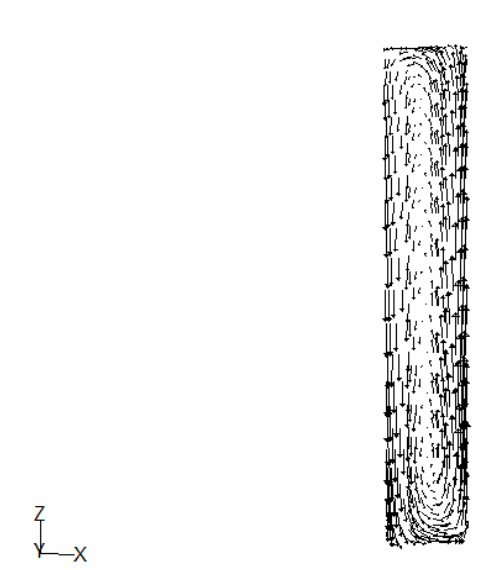

Figure 4-22: Vectors of velocity in cylinder

The simulation shows that the temperature difference alone conduce small fluid velocities in a closed volume.

5 DISCUSSION

A summary of the simulation results is collected in Table 5-1. Considering a hydrate equilibrium temperature of 20 ^{o}C, only tree of the eight cases reaches this temperature.

Table 5-1: Summary of results

Case	*Orientation*	*HTC [W/m^{2}K]*	*Average T [^{o}C]*	*End T [^{o}C]*	*HET reached after:*
1a	vertical	580	30	14	1.40 m (≈6D_i)
1b	vertical	1100	30	16	1.42 m (≈6D_i)
2a	horizontal	580	41	38	
2b	horizontal	1100	40.5	36	
3a	vertical	580	40	24	
3b	vertical	1100	35	12	1.51(≈6.3D_i)
4a	horizontal	580	50	44	
4b	horizontal	1100	48	40	

The term D_i (inner diameter) is used to describe positions of the cross section planes in the deadleg. Figure 5-1 shows the position of the planes.

Figure 5-1: Cross section planes in deadleg

5.1 Evaluation of grid

The grid was divided into different zones to satisfy different requirements. A grid as structured as possible was desired to make convergence easier. The inlet section of the pipe is a straight pipe with a length equal to 20 D_i. This length was chosen to ensure a fully developed flow upstream the branch. This section of the pipe has a boundary layer and descending length of cells. The T-bend is meshed separately and here is where the smallest cells are located. It was necessary to mesh the T-bend separately to avoid skewness in the mesh. The branch has a fine mesh. This is the critical part of the system regarding heat transfer. The steel section is meshed with a coarse mesh since the heat transfer is linear through the wall. The grid was examined in Gambit and the worst element has a quality value of 0.98.

According to [8] the y^+ value >30 is recommended for a Re ≥15000. The y^+ value for the main pipe calculated in Fluent is 85 for the 2.2 m/s cases and 310 for the 9 m/s cases. The y^+ value in the deadleg is plotted for each cross section plane in the deadleg, see Figure 5-2. The minimum value is 30, which is the minimum recommended y^+ value when turbulence is modeled by the k-ε model.

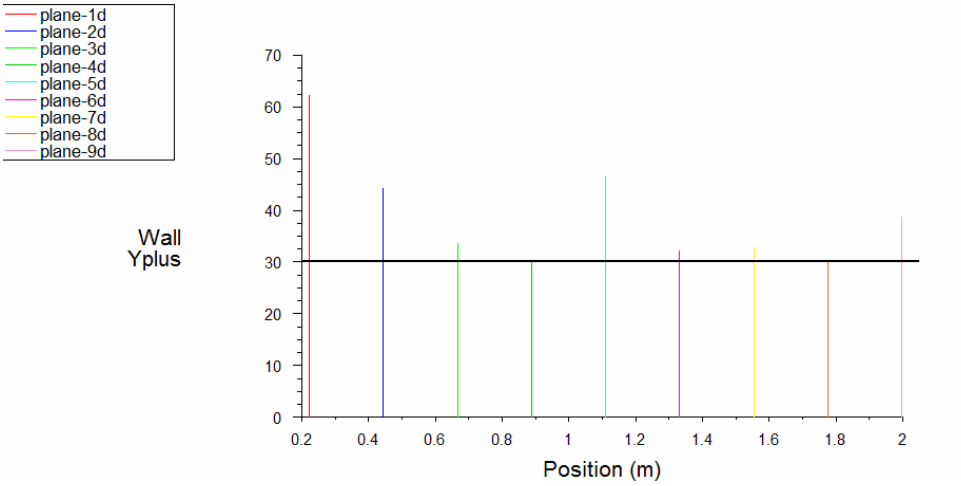

Figure 5-2: y^+ values, cross section planes in deadleg, case 1a

5.2 Temperature distribution

Case 1a, which is a vertical oriented deadleg, has an average temperature of 30 ^oC. This temperature is calculated from a Fluent xy-plot along the centerline. In the first part of the deadleg the temperature is almost stable. After approximately $3D_i$ the temperature decreases rapidly and crosses the HET at a length of 1.40 m into the deadleg, see Figure 4-5. As the orientation is changed to horizontal in case 2a, the average temperature is increased to 41 ^oC. The temperature gradient is smaller and the temperature difference through the deadleg is 16 degrees. The difference in the temperature profiles for the vertical and horizontal implies a more uniform flow field for the horizontal case. This could be due to gravity and that gravity force is less important for the horizontal deadleg. When the main stream velocity is increased to 9 m/s in cases 3 and 4, the average temperature is considerably increased. Case 4a, the horizontal setup has the highest average of 50 ^oC, with a temperature drop along the centerline of 15 degrees.

5.3 Flow field and velocity

To investigate the flow velocity in the deadleg the velocity along the center and wall lines are plotted with xy-plot function in Fluent for case 1a and 2a. The average values are calculated from those data, see Table 5-2.

Table 5-2: Average velocities for case 1a and 2a

Case	*Average velocity center [m/s]*	*Average velocity wall [m/s]*
1a	0.1015	0.1556
2a	0.0838	0.1427

There is no significant difference in the average velocity of these two cases. Both cases have about the same inlet and end velocity, but the velocity of case 1a is more fluctuating.

Figure 5-3 shows the velocity profile of the center and wall line for a vertical case. Circulating vortexes are formed immediate, and the velocity fluctuates between positive and negative direction through the whole length of the deadleg. This will prevent new, warm gas from the main pipe replacing the cold gas.

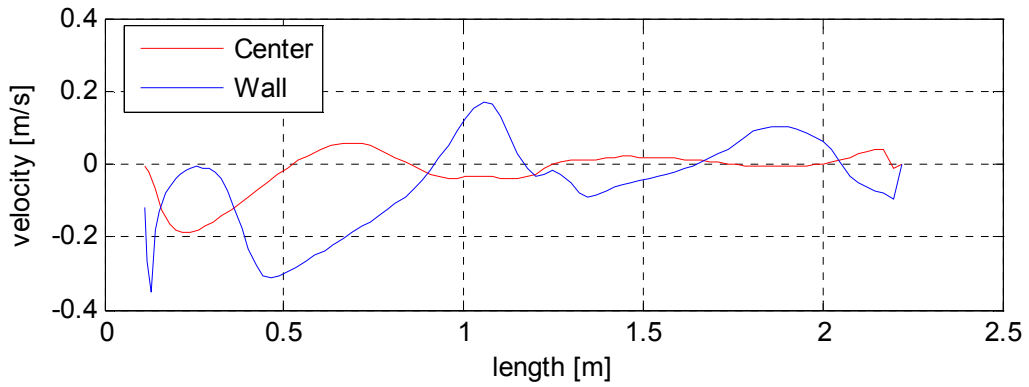

Figure 5-3: y-velocity, case 1a

Figure 5-4 is a sketch of the y-velocity and shows the changes in direction for the center and wall lines.

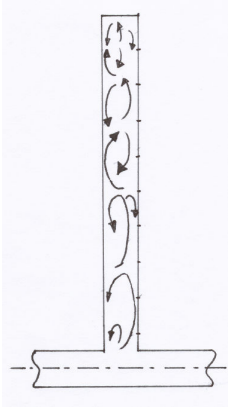

Figure 5-4: Sketch of y-velocity flow pattern in vertical deadleg

Figure 5-5 shows the velocity profile of the center and wall line. The velocity is negative in the first part of the deadleg. At approximately 0.75 m a circulating cell or vortex is established with a positive (outward) flow direction close to the wall and a negative (inward) flow in the center of the deadleg. This results in a more stable flow pattern and transport of heat outwards in the deadleg.

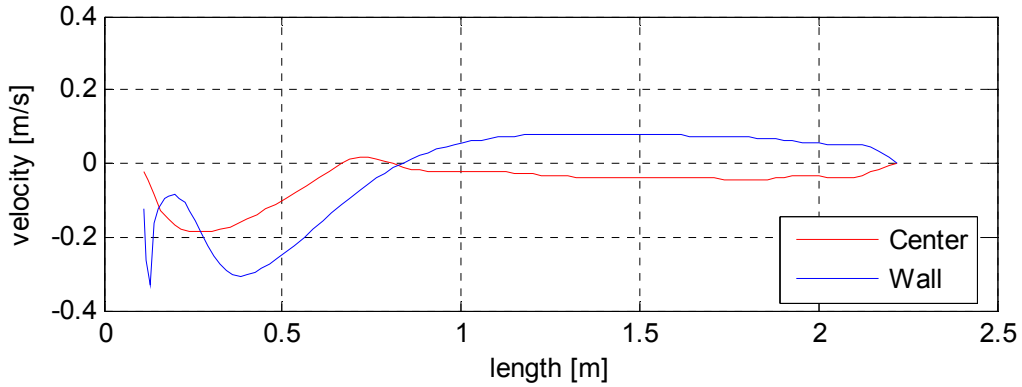

Figure 5-5: y-velocity, case 2a

The flow pattern for the 9 m/s cases is similar to the 2.2 m/s cases. See appendix C. Figure 5-6 is a sketch of the flow pattern along the wall and center. A continuous transport of heat and replacement of gas outwards in the deadleg maintains the temperature above the HET.

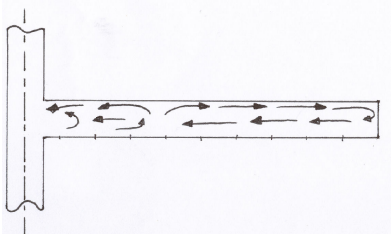

Figure 5-6: Sketch of y-velocity flow pattern in horizontal deadleg

To achieve a better understanding of the flow field in the y-direction, a surface integral of the average vertex velocity is calculated in Fluent, see Table 5-3. The circular cross section planes represent the length of a D_i, see Figure 5-1. For case 1a, this velocity changes direction several times. This is in accordance with the velocity profile in Figure 5-3. For case 2a, the average vertex velocity is positive for all planes. A possible explanation for the direction changes in the vertical deadleg could be that the vortexes created by buoyancy will smooth out or work against the vortexes driven by the flow in the main pipe. The result is that heat loss to the environment is larger and without replacement of the gas, the temperature drops abruptly. The vertical deadleg is more vulnerable than the horizontal.

Table 5-3: Average vertex velocity cross section planes

Plane	***Case 1a [m/s]***	***Case 2a [m/s]***
$1D_i$	-0.012	0.046
$2D_i$	0.011	0.028
$3D_i$	-0.009	0.006
$4D_i$	0.001	0.007
$5D_i$	0.008	0.011
$6D_i$	-0.003	0.010
$7D_i$	-0.001	0.010
$8D_i$	0.001	0.009
$9D_i$	-0.003	0.007
$10D_i$	0	0

5.4 Effect of heat transfer coefficient

The two heat transfer coefficients used as boundary conditions in the simulations are corresponding to sea water velocities of roughly 0.2 and 0.5 m/s. The simulations where preformed to investigate the sensitivity of varying sea water conditions. For the low velocity cases this seems to be of less importance. The average temperature is equal for both 1a and 1b, and 2a and 2b, see Table 5-1. The temperature at the end is two degrees lower for both 1b and 2b. There is no significant difference in the temperature distribution of the two cases. For case 3a and 3b, the difference of both average and end temperatures are lower in case 3b, respectively 5 and 12 degrees. For case 4a and 4b the difference of both average and end temperatures are

lower in case 4b, respectively 2 and 4 degrees. The effect of a higher HTC is not that significant as the effect of varying flow field and velocity.

5.5 Buoyancy

The simulations of buoyancy were performed to investigate the velocities induced from free convection. Fluent recommends the Boussinesq model as equation of state or a transient approach for free convection cases [13]. Several model setups where considered, but convergence was difficult to achieve. This was for both the transient and steady solver. The non-compressible ideal-gas was the final choice of equation of state. The results of the buoyancy simulations must be regarded as a hint of the flow pattern. The common observation for all the different simulation setups is that the maximum fluid velocity is in the range of 0.15-0.20 m/s.

6 CONCLUSION

Hydrate formation in hydrocarbon production systems is a well known challenge for the oil and gas industry. There are a number of challenges connected to hydrates and subsea production, and this report is a computational and analytical study of hydrate formation in subsea deadlegs. The investigation of heat transfer and flow field in subsea deadlegs has been done the by following approach

- A review of literature on heat transfer and subsea hydrates
- A three dimensional T-bend geometry with mesh has been created in Gambit
- Eight CFD simulations has been preformed in Fluent, four vertical and four horizontal oriented cases
- Analyzing the results with respect to temperature and velocity. The horizontal deadleg is more robust and has a higher temperature than the vertical and that the hydrate equilibrium temperature was reached in only three of the eight cases
- A study of a closed cylinder. The geometry and mesh was created in Gambit, and simulations to investigate the effect of buoyancy was performed in Fluent. The results shows a velocity driven from free convection in the range of 0.15-0.20 m/s

To be able to define a design criterion and recommended length of deadlegs, this problem should be further investigated.

REFERENCES

[1] Incropera FP, DeWitt DP, *Fundamentals of Heat and Mass Transfer*, Fifth edition

John Wiley & Sons, USA, 2002

[2] Geankoplis JC, *Transport Processes and Separation Process Principles*, Fourth edition, PRENTICE HALL, USA, 2003

[3] Musakaev NG, Urazov RR, Shagapov VSh, *Hydrate formation kinetics in piped natural-gas flows,* Thermophysics and Aeromechanics, Vol. 13, No. 2, 2006

[4] Guðmundsson JS, *Prosessing of petroleum,* Kompendium NTNU 2007

[5] Su J, Cerqueira DR, Estefen SF, *Simulation of Transient Heat Transfer of Sandwich Pipes With Active Electrical Heating,* Journal of offshore and artic engineering, ASME, New York, 2005

[6] Moe R, Sørbye S, Skogen K, Lofseik C, *A comparisoion of experimental data and CFD predicted cool down in subsea equipment*, Fourth International Conference on CFD in the Oil and Gas, Metallurgical & Process Industries, SINTEF/NTNU, Trondheim 2005

[7] Habib MA, Said SAM, Badr HM, Hussaini I, *Effect of geometry on flow field and oil/water separation in vertical deadlegs,* International journal of numerical methods for heat and fluid, 2005

[8] Versteeg HK, W Malalasekera, *An introduction to Computational Fluid Dynamics*, Pearson Education Limited, England, 1995

[9] Habib MA, Said SAM, Badr HM, Hussaini I, *On the Development of Criterion,* Journal of fluids engineering, ASME New York, 2005

[10] Solbakken S, Multiphase Systems and Flow Assurance, Statoil ASA. E-mail and report received March 2007

[11] Sea water properties collected at:
http://www.kayelaby.npl.co.uk/general_physics/2_7/2_7_9.html

[12] Kvingedal B, department of Metocean, Mapping and Geotechnics, Statoil ASA. E-mail received April 2007

[13] FLUENT 6 User's Guide, volume 1-5, December 2001

[14] Statoil internal documentation and procedures

[15] Statoil's piping and valve material specifications collected at:
http://tr2000.statoil.com/TR2000

[16] Habib MA, Said SAM, Badr HM, Mokheimer EMA, Hussaini I, Al-Sanaa M, *Characteristics of flow field and water concentration in a horizontal deadleg*, Heat and Mass Transfer, Springer-Verlag, 2004

LIST OF APPENDIX

APPENDIX A:

F4203 Master Thesis

Title: **Computational study of heat transfer in subsea dead-legs for evaluation of possible hydrate formation.**

Student: Hilde Andersen

College supervisor: Knut Vågsæther

External partners: Audun Faanes, Statoil ASA, Rotvoll

Task description:

A case-study of the Tordis IOR (Increased Oil Recovery) will be performed to achieve knowledge and process parameters of subsea systems.

The candidate will make a literature review on heat transfer and flow patterns due to natural convection with focus on subsea deadlegs. Analytical analysis of these effects will be carried out.

CFD (Computational Fluid Dynamics) analysis of heat transfer effects and evaluation of the possibility of hydrate formation in subsea deadlegs will be carried out.

Task background:

Hydrate formation in hydrocarbon production systems is a well known challenge for the oil and gas industry. Hydrate formation is commonly avoided in order to minimize the probability of production loss, equipment damage/integrity and personnel injuries. Maintaining the process fluid temperature above a threshold-value, referred to as the hydrate equilibrium temperature, effectively protects the system from hydrate formation. Subsea production systems are generally more exposed due to unfavourable ambient conditions, i.e. cold surroundings and sea currents which favour a large heat loss. Deadlegs, i.e. piping without through-put, are of special concern since fluid temperatures in such devices typically drops abruptly towards the dead-end. It is of crucial importance to keep dead-legs above the hydrate formation temperature during production. Deadlegs are commonly found in relation with chemical injection lines and on manifolds. Future subsea production systems will increase in complexity, and accordingly more deadlegs will be introduced in such systems. From a hydrate-protection point of view this is challenging. The design of subsea production systems involving deadlegs should as far as possible be governed by hydrate-protection requirements to minimize hydrate related problems. In order to achieve an improved design of deadlegs more knowledge regarding the temperature distribution in deadlegs is needed.

APPENDIX B:

Fluent input data		
Turbulence model	Standard k-ε	
Energy equation	Yes	
Operating conditions	10^7 Pa, 338 K	
Boundary conditions	*Mass flow inlet*	6, 26 kg/s
	Pressure outlet	0 Pa gauge
	Valve	wall, convection heat coeff. 580 W/m^{2}K, free stream temperature 280 K
	Outside wall	wall, convection heat coeff. 580 W/m^{2}K, free stream temperature 280 K
	Materials	methane, steel
Solver	Segregated	
Scheme	Second order	
Mesh	Structured, 204024 cells	
Convergence criterion	10^{-5}	

APPENDIX C:

Material properties					
	ρ [kg/m^3]	*k [W/m·K]*	*Cp [J/kg·K]*	*MW [kg/kmole]*	*μ [kg/m·s]*
Steel	7850	20	460	-	-
Insulation	600	0.12	1250	-	-
Fluid	Ideal gas	0.0463	2865	21	$1.56 \cdot 10^{-5}$

APPENDIX D:

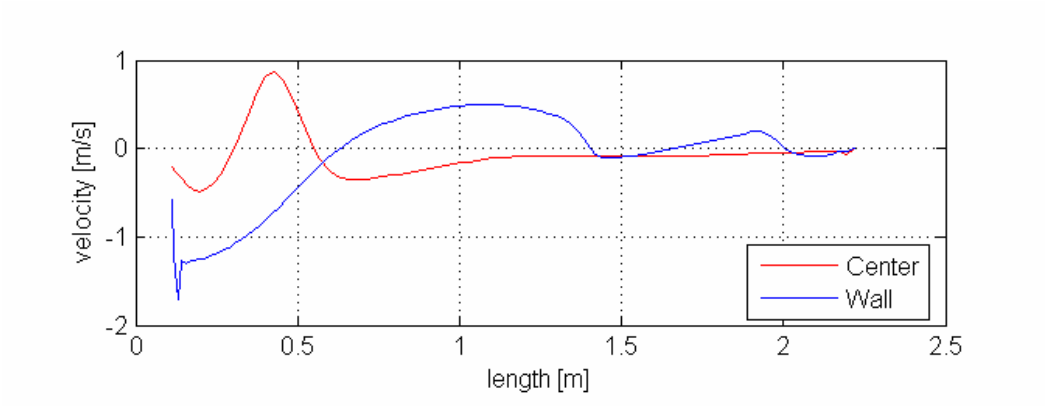

y-velocity, case 3a

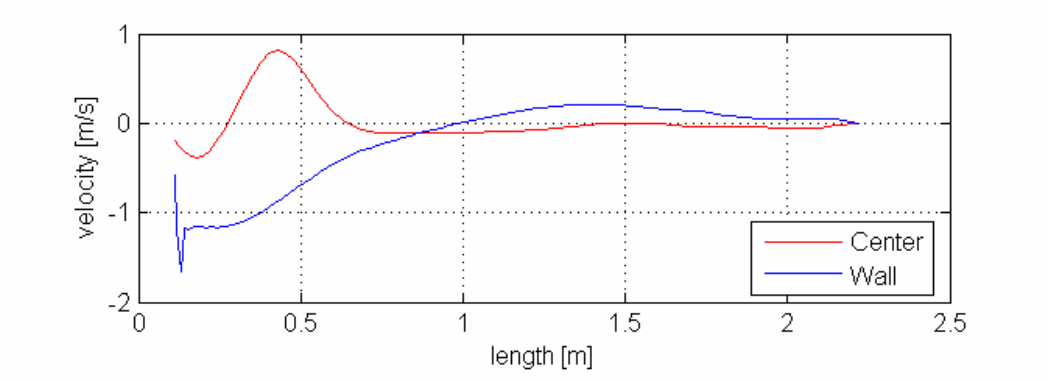

y-velocity, case 4a